CHAPTER SIX
FLUID GEOCHEMISTRY AND PROVENANCE

6.1 INTRODUCTION

Alteration and mineralization assemblages are the product of early potassic and silicic alteration, and later carbonation and associated base and precious metal mineralization, as part of a single, extended episode during active faulting. These assemblages only indicate the general characteristics and evolution of the hydrothermal fluid. More specific aspects of fluid geochemistry, such as solute and solvent types and concentrations, and physical conditions at various stages in the evolution of the fluid must come from studies of relict fluid, preserved as inclusions trapped in the alteration phases, from studies of mineral-fluid equilibria, and from stable isotope studies.

A series of complementary studies was undertaken to characterize some of the chemical features of the hydrothermal fluid. Petrographic examination of inclusions hosted by quartz identified the different inclusion populations and their paragenetic sequence, and also provided qualitative information on inclusions compositions. Daughter phases were identified using a combination of optical properties and semi-quantitative SEM X-ray spectral analysis. The results guided subsequent studies.

Estimates of near-primary fluid composition were obtained by measuring the volumes of liquid, vapour and daughter phases in a population of primary fluid inclusions. Published salt solubility data were then used to approximate the overall fluid chemistry of the homogeneous fluid (*i.e.* at the time of trapping). Reconnaissance microthermometric measurements of eutectic, final melting and homogenisation temperatures of phases in inclusions from the different populations provided fluid compositional information for inclusions without solid phases, and also estimates of

physical conditions of trapping (and hence of alteration and mineralization). Stable isotope studies of alteration phases were used to calculate fluid stable isotope compositions, and hence constrain interpretations of the possible sources of components comprising the hydrothermal fluid.

6.2 FLUID INCLUSION CHARACTERIZATION

6.2.1 Introduction

A reconnaissance survey of ten samples containing good examples of a range of primary and pseudosecondary fluid inclusions revealed several different populations. The broad physical and chemical characteristics of each population and their paragenetic sequence have been established using microthermometry, allowing preliminary interpretation of the nature of the primary fluid, and the subsequent chemical and thermal evolution of this fluid. Estimates of fluid trapping temperatures also constrain the isotope results.

Fluid inclusions of useable size (>10 μm) are only regularly present in quartz, though in rare instances vein-infill carbonate has trapped resolvable inclusions. The petrographic features of both types are documented below, but thermometric and volumetric measurements were made only on the more ubiquitous examples from quartz. Inclusions are classified on the basis of contents, as suggested by Shepherd *et al.* (1985). The paragenesis is determined by interpretation of individual inclusions as primary, pseudosecondary or secondary, following the criteria of Roedder (1984, pp.43-45). Table 6.1 summarizes the characteristics of the different classes. Details of thermometric techniques and complete data are recorded in Appendices C and F1.

TABLE 6.1: Summary of the main characteristics of different populations of fluid inclusions in quartz from the Mount Dore system.

Inclusion Type	**Essential phases**	**Style of occurrence**	**Size**	**"Generation"**
Type I multiphase solid	$\geq$ 3 solids + liquid + vapour	irregular, 3D aggregates; isolated inclusions	$\leq$ 15 μm	primary
Type II multiphase solid	1 solid + liquid + vapour	discontinuous regular to irregular planes	$\leq$ 5 μm	primary-pseudosecondary
Immiscible liquid	CO_2-rich liquid $\pm$ gaseous CO_2 $\pm$ aqueous liquid	discontinuous, irregular planes; isolated inclusions	$\leq$ 10-15 μm	primary
Type I liquid-rich, two-phase	liquid >> vapour	widely-spaced planes	$\leq$ 10-15 μm	pseudosecondary
Type II liquid-rich, two-phase	liquid >> vapour	densely packed planes	$\leq$ 2 μm	secondary
Vapour-rich, two-phase	vapour + liquid (variable ratio)	discontinuous irregular planes; isolated inclusions	$\leq$ 10-15 μm	primary-pseudosecondary
Solid inclusions	1 solid $\pm$ liquid $\pm$ vapour	irregular, 3D aggregates; discontinuous planes	$\leq$ 5 μm	primary

6.2.2 Type I multiphase solid

General characteristics

These inclusions occur either in irregular three-dimensional aggregates in the central regions of grains, or as isolated, or trains of isolated, inclusions in quartz (Figure 6.1 a-d). They range in size from 15 μm to below the resolution of the microscope, and generally have irregular shapes, though some show crude "negative-crystal" forms. They invariably have at least three, commonly up to five, and rarely up to eight daughter minerals, occupying an average of about 30 volume percent of the inclusion.

Type I multiphase solid inclusions are primary in the sense of Roedder (1984), and therefore contain fluid closest to the original composition, although this fluid is that present after the bulk of the K-metasomatism (since the quartz host for the inclusions precipitated after the K-feldspar). The composition of this "primary" fluid was estimated from phase volumetric measurements of the contents of twenty-eight inclusions of this type (Section 6.3).

Daughter phases

Tentative daughter identification was done using optical properties (Table 6.2), and semi-quantitative SEM X-ray spectral analysis confirmed the presence of the identified phases (see Appendix C for SEM analytical technique). Daughters invariably present are halite, sylvite and iron-chloride. Calcite (or dolomite) is also usually present, and haematite is also common. Ca-chloride is present rarely (Table 6.3).

Halite is characteristically cubic, colourless to pale yellow, or rarely pale, speckly orange-red, with moderate to high relief relative to that of the solution, but similar refractive index to the quartz host (mutual contacts are virtually invisible). It is differentiated from sylvite mainly on the basis of relief. Large cubic daughters in opened inclusions gave strong Na and Cl X-ray peaks (*e.g.* Figures 6.2a, 6.3a).

FIGURE 6.1: Photomicrographs of examples of different types of fluid inclusions observed in the Mount Dore deposit. All inclusions illustrated here are hosted by quartz, except for those depicted in (i), which occur in carbonate. Scale is indicated.

(a) Three dimensional aggregate of Type I multiphase solid inclusions in the centre of a crystal of quartz infill (JCU-27086).

(b-d) Examples of individual Type I multiphase solid inclusions. **A** - antarcticite; **C** - carbonate; **F** - Fe-chloride; **H** - halite; **L** - liquid; **S** - sylvite; **U** - unknown daughter; **V** - vapour (all are from JCU-27273).

(e) Trail of Type II multiphase solid inclusions. **H**, **L** and **V** as previously noted (JCU-27163).

(f) Example of immiscible fluid inclusion. CO_2 vapour is contained within an enclave of liquid CO_2, and both are surrounded by aqueous liquid (JCU-27163).

(g) Pair of immiscible fluid inclusions. The larger one contains several daughter phases in the aqueous liquid (JCU-27068).

(h) Trail of Type I liquid-rich two-phase fluid inclusions, having approximately constant liquid:vapour ratio, in association with planes of very tiny Type II liquid-rich two-phase inclusions (JCU-27273).

(i) Elongate Type I liquid-rich two-phase inclusions hosted by carbonate. Preferred orientations are probably crystallographically controlled (JCU-27131).

(j) Wide field of view showing a host of primary, pseudosecondary and secondary inclusion types (JCU-27199).

(k) Narrow planes of Type II liquid-rich two-phase ("secondary") inclusions cutting an otherwise relatively clear field of view. Note the relatively large Type I multiphase solid inclusions scattered sparsely throughout (JCU-27273).

(l) Trail of vapour-rich inclusions crossing a field of view heavily dusted with a variety of other inclusion types (JCU-27218).

(m,n) Examples of probable solid inclusions of halite in quartz. Their presence is revealed by thin films of aqueous liquid around their margins. (m) is from JCU-27265; (n) is from JCU-27096.

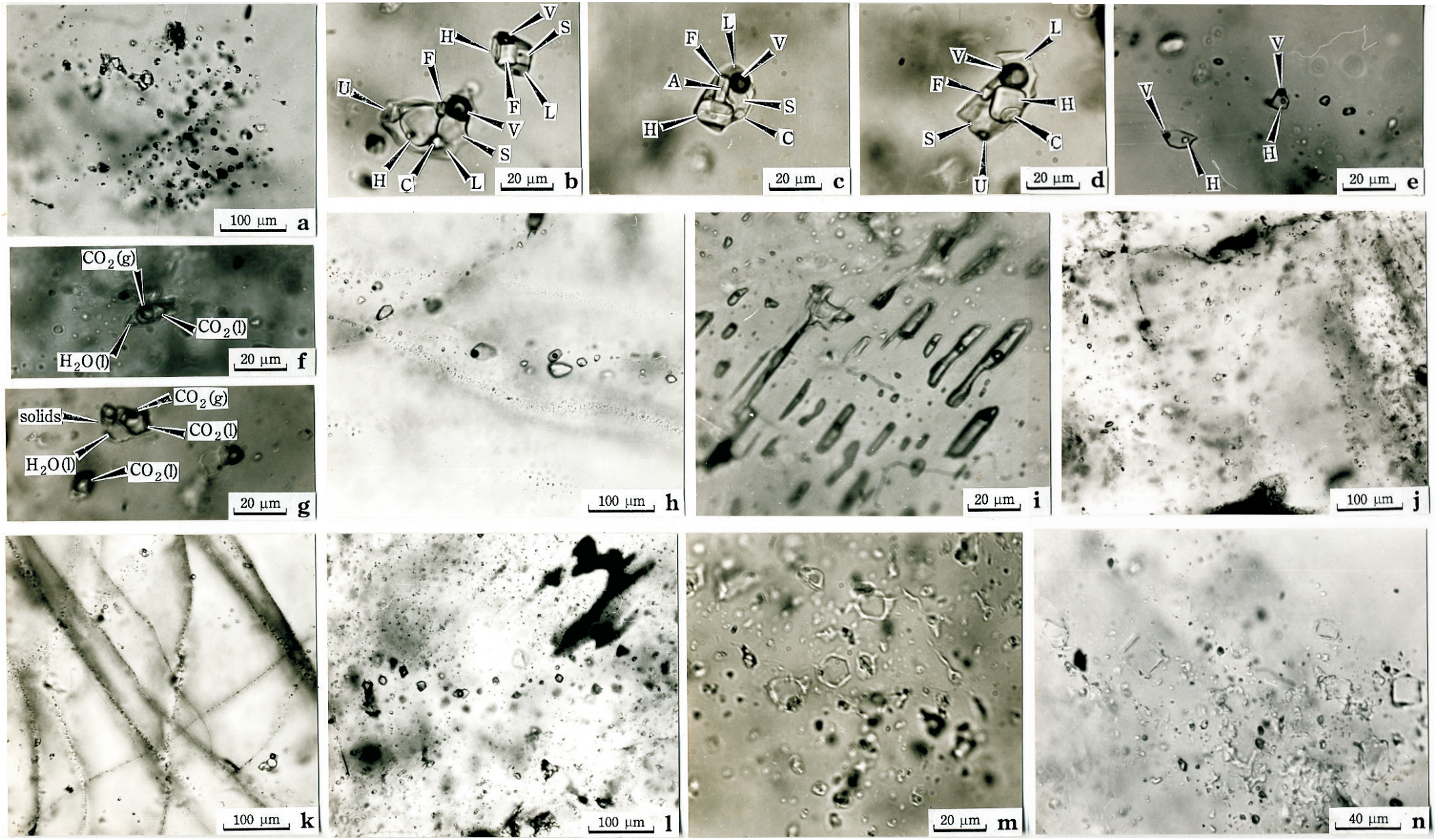
100 µm a
V S H F U F L V S H C L 20 µm b
L F V A S H C 20 µm c
L V F H S C U 20 µm d
V V H H 20 µm e
CO2 (g) CO2 (l) H2O (l) 20 µm f
CO2 (g) solids CO2 (l) H2O (l) CO2 (l) 20 µm g
100 µm h
20 µm i
100 µm j
100 µm k
100 µm l
20 µm m
40 µm n

TABLE 6.2: Optical properties of the identified daughter phases in Type I multiphase solid inclusions. Hyphen indicates an optical property which was not observed.

Name	**Composition**	**Habit**	**Comparative relief**		**Colour**	**Birefringence**
			fluid	***host***		
Halite	NaCl	cubic	high	low	colourless, pale yellow or orange-red	isotropic
Sylvite	KCl	cubic	low	high	colourless	isotropic
Iron chloride	$FeCl_2.2H_2O$	tabular (often rhombic/hexagonal)	moderate	-	pale yellow-green	moderate-high
Carbonate	$CaCO_3$ or $CaMg(CO_3)_2$	rhombohedral?	low-high	-	colourless	very high
Haematite	Fe_2O_3	platy	moderate	-	red-orange	-
Antarcticite	$CaCl_2.6H_2O$	acicular	moderate	-	colourless	moderate

TABLE 6.3: List of daughter phases identified in Type I multiphase solid inclusions used in volumetric studies. Question mark indicates tentative identification. *Abbreviations:* **hal** - halite; **syl** - sylvite; **Fe-chl** - $FeCl_2.2H_2O$; **carb** - calcite or dolomite; **haem** - haematite; **ant** - antarcticite ($CaCl_2.6H_2O$)

SAMPLE AND LOCALITY	INCLUSION NUMBER	DAUGHTERS
JCU-27068 SMD-76-01 44.65 m	4	hal, syl, Fe-chl, carb, 1 unknown
JCU-27086 SHQ-76-13 53.95 m	1	hal, syl, Fe-chl, carb, 1 unknown
	5	hal, syl, Fe-chl, carb
	9	hal, syl, Fe-chl, carb
	10	hal, syl, Fe-chl, carb
	11	hal, syl, Fe-chl, carb, 1 unknown
JCU-27094 SHQ-77-16 134.15 m	1	hal, syl, Fe-chl, carb, haem, 1 unknown
	7	hal, syl, Fe-chl, carb, 1 unknown
	10	hal, syl, Fe-chl, carb, ?haem, 1 unknown
	11	hal, syl, Fe-chl, carb
	12	hal, syl, Fe-chl, carb, haem, 1 unknown
JCU-27110 SHQ-77-19 283.75 m	1	hal, syl, Fe-chl, ?carb
	2	hal, syl, Fe-chl, 1 unknown
	3	hal, syl, Fe-chl, carb
	4	hal, syl, Fe-chl, carb
JCU-27199 SHQ-78-27 266.7 m	1	hal, syl, Fe-chl, ?carb
	2	hal, syl, Fe-chl, 2 unknowns
	3	hal, syl, Fe-chl, ?haem
	6	hal, syl, Fe-chl
	9	hal, syl, ?Fe-chl
JCU-27271 SHQ-79-40 281.9 m	1	hal, syl, Fe-chl
	4	hal, syl, Fe-chl, ?carb, ?1 unknown
	9	hal, syl, Fe-chl, 2 unknowns
JCU-27273 SHQ-79-40 282.95 m	1	hal, syl, Fe-chl, carb, ?haem, ant
	4	hal, syl, Fe-chl, carb, ?ant
	5	hal, syl, Fe-chl, carb, haem, ant, 1 unknown
	8	hal, syl, Fe-chl, carb, 1 unknown
	10	hal, syl, Fe-chl, carb

Sylvite was identified as a cubic, colourless phase, with much lower (comparable) relief in the solution than halite. Where halite and sylvite occur together in the same inclusion, sylvite was the smaller of the two and had a slightly less well-defined habit (eg. Figure 6.1b-d). Cubic daughters yielding strong K and Cl X-ray peaks were observed using SEM (*e.g.* Figure 6.3b,c)

Fe-chloride occurs as stubby to elongate, platy to prismatic crystals, sometimes with six-sided cross-sections (*e.g.* Figure 6.2c,d). Relief is moderate to high relative to the liquid, pleochroism is a pale green-yellow, and birefringence is a strong pale blue to pale green. SEM scans of daughters showing this habit yielded strong Fe and Cl peaks (Figure 6.3c). Small daughters were sometimes observed spatially associated with the Fe-chloride phase during these scans. These solids showed K peaks in addition to Fe and Cl, suggesting the presence of K-Fe-chlorides (Figure 6.3d). These may have been present in the unopened inclusion, but may instead have precipitated when the fluid vaporized on opening of the inclusion.

Fe-chloride commonly occurs as a hydrated species, and the hydration factor is required for volumetric calculations. In the "simple" $FeCl_2$-H_2O system Fe-chloride occurs as a tetrahydrate up to 76.5^oC; above this temperature it is a dihydrate (Schimmel, 1928). $FeCl_2.4H_2O$ is pale bluish green to light blue in plane polarized light, and only weakly birefringent. $FeCl_2.2H_2O$ is green to colourless, needle-like and strongly birefringent (Winchell and Winchell, 1964). The Fe-chloride observed in this study has optical properties consistent with the dihydrate form (Table 6.3). Interpretation of the Fe-chloride phase as the dihydrate form may be erroneous, firstly because of its existence outside its "normal" stability range, and also because the phase observed in this study dissolved (with difficulty) only at relatively high temperatures (>350^oC). The solubilities of Fe-chlorides in pure water are very high (greater than 80 weight percent at temperatures less than 100^oC; Potter and Clynne, 1978). However, the solubility behaviour of Fe-chloride (or any salt) in multi-component systems is poorly constrained. The presence of highly soluble salts such as $MgCl_2$ (and probably $CaCl_2$?) in the fluid is known to lower the transition temperature between the tetrahydrate and dihydrate forms (Boecke, 1911), and the presence of other ions in

FIGURE 6.2: Annotated SEM photomicrographs of opened Type I multiphase solid inclusions, showing examples of different daughter phases. Elements identified in X-ray spectra are listed in square brackets next to each phase. Some of the solids may be sublimates, precipitating from solution as the liquid evaporated. Scale is indicated.

(a) halite (**H**) and Fe-chloride (**F**)
(b) sylvite (**S**) and halite (**H**)
(c) sylvite (**S**), halite (**H**) and Fe-chloride (**F**)
(d) Fe-chloride (**F**) and halite (**H**)
(e) carbonate (**C**) and Ca-chloride (**A**)
(f) haematite (**Hm**)

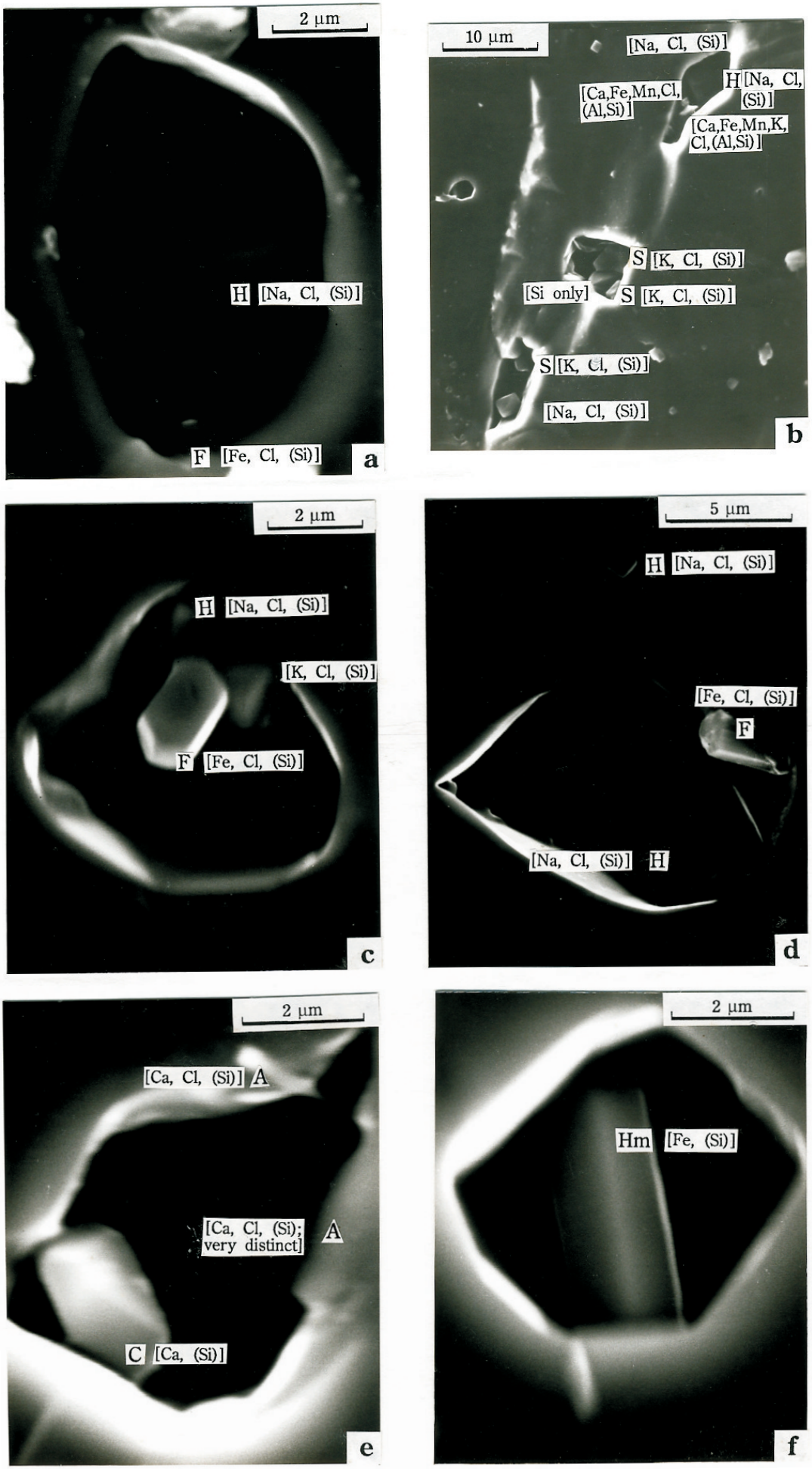
2 µm
H [Na, Cl, (Si)]
F [Fe, Cl, (Si)]
a
10 µm
[Na, Cl, (Si)]
[Ca,Fe,Mn,Cl, (Al,Si)]
H [Na, Cl, (Si)]
[Ca,Fe,Mn,K, Cl,(Al,Si)]
S [K, Cl, (Si)]
[Si only]
S [K, Cl, (Si)]
S [K, Cl, (Si)]
[Na, Cl, (Si)]
b
2 µm
H [Na, Cl, (Si)]
[K, Cl, (Si)]
F [Fe, Cl, (Si)]
c
5 µm
H [Na, Cl, (Si)]
[Fe, Cl, (Si)]
F
[Na, Cl, (Si)] H
d
2 µm
[Ca, Cl, (Si)] A
[Ca, Cl, (Si); very distinct] A
C [Ca, (Si)]
e
2 µm
Hm [Fe, (Si)]
f

FIGURE 6.3: Characteristic X-ray spectra of daughter phases in Type I multiphase solid inclusions. Phase identities and sample numbers are indicated on each spectrum. Note that all spectra have Si peaks, derived from the quartz host.

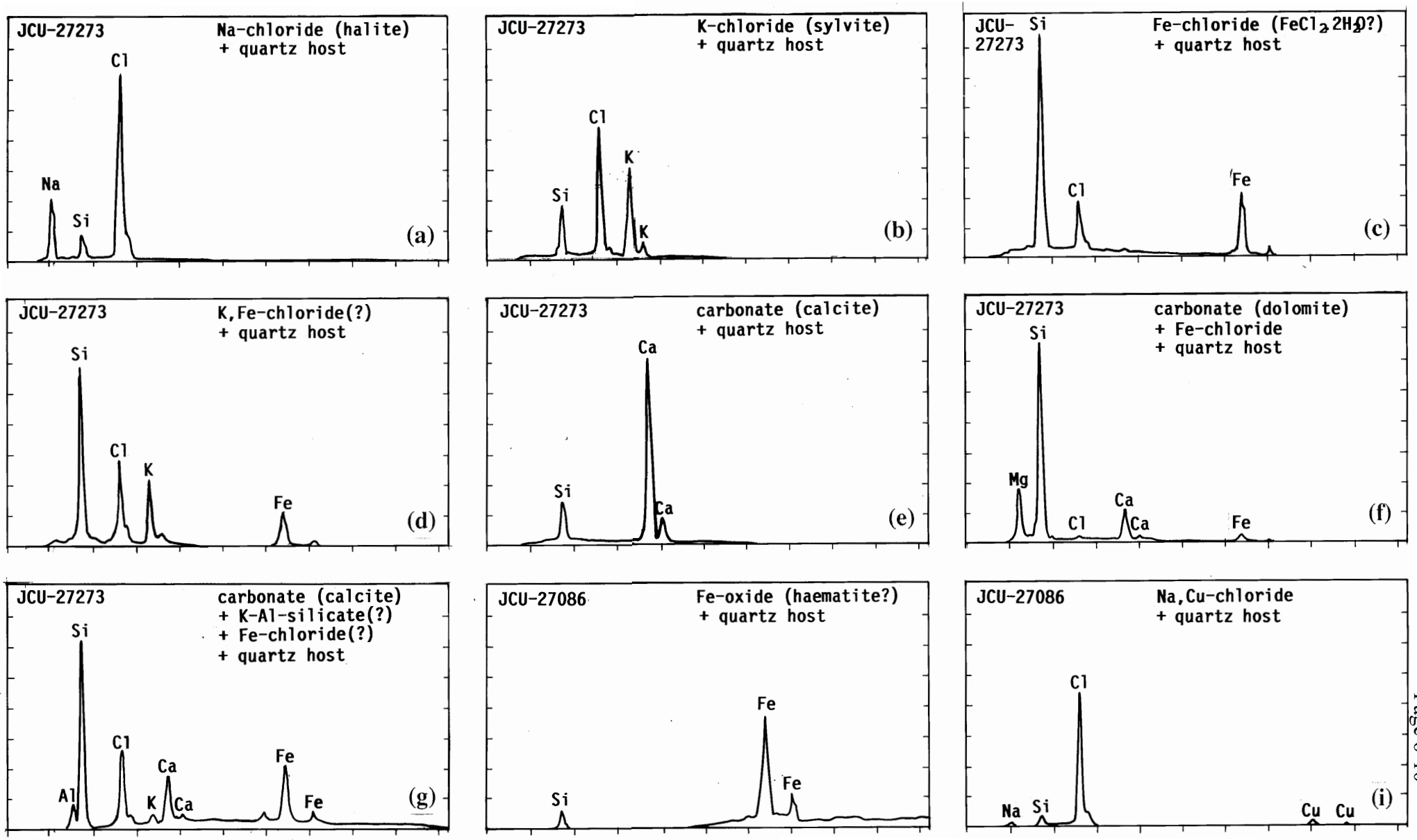
JCU-27273
Na-chloride (halite)
+ quartz host
Cl
Na
Si
(a)
JCU-27273
K-chloride (sylvite)
+ quartz host
Cl
K
Si
K
(b)
JCU-27273
Fe-chloride (FeCl2.2H2O?)
+ quartz host
Si
Cl
Fe
(c)
JCU-27273
K,Fe-chloride(?)
+ quartz host
Si
Cl
K
Fe
(d)
JCU-27273
carbonate (calcite)
+ quartz host
Ca
Si
Ca
(e)
JCU-27273
carbonate (dolomite)
+ Fe-chloride
+ quartz host
Si
Mg
Cl
Ca
Ca
Fe
(f)
JCU-27273
carbonate (calcite)
+ K-Al-silicate(?)
+ Fe-chloride(?)
+ quartz host
Si
Cl
Ca
Fe
Al
K
Ca
Fe
(g)
JCU-27086
Fe-oxide (haematite?)
+ quartz host
Fe
Si
Fe
JCU-27086
Na,Cu-chloride
+ quartz host
Cl
Na
Si
Cu
Cu
(i)

solution may account for the low-temperature occurrence of $FeCl_2.2H_2O$. Extra ions, and other factors such as persistent leakage of liquid from inclusions during heating could explain the apparently low solubility. The dihydrate form is retained in subsequent volumetric studies.

Small, very high relief, high (white) birefringence daughters occasionally showing a rhombic habit are identified as carbonate (*e.g.* Figure 6.2e). Both calcite and dolomite occur in the alteration assemblage, and during the SEM scans daughters were identified which yielded Ca peaks only (*e.g.* Figure 6.3e), and which yielded both Ca and Mg peaks (Figure 6.3f).

Haematite was identified as small, red-orange (PPL), platy flakes with rounded corners, inconsistently present in some of the Type I multiphase solid inclusions. A platy phase located in the SEM studies yielded Fe peaks only (Figures 6.2f, 6.3h), and the platy habit suggests an oxide rather than a carbonate. Haematite may be a foreign inclusion, transported as a suspended phase in the fluid.

Very small (volumetrically insignificant), acicular crystals occurring in groups of two or three were observed in rare instances. These are tentatively identified as calcium chloride because optical properties are consistent with this phase (Table 6.3; Potter and Clynne, 1978; Phillips and Griffen, 1981), and because the thermometric study suggested the presence of abundant Ca^{2+} in solution. The hexahydrate form of Ca-chloride (antarcticite) is preferred, because experimental studies of the $CaCl_2$-NaCl-KCl-H_2O system at 25^{o}C show this to be the dominant form (Yanatieva, 1946). Acicular to platy daughters with strong Ca and Cl peaks were definitely identified in two of the inclusions studied using the SEM (*e.g.* Figure 6.2e).

Thermometry

Highly saline inclusions proved difficult to work with, because they invariably decrepitated before homogenization to a single fluid phase. Even in the absence of

catastrophic decrepitation, attempts to confirm vapour homogenization temperatures commonly yielded higher values in repeat runs, indicating gradual leakage of liquid from submicroscopic fractures. Despite these shortcomings, some significant observations were made.

In inclusions where both transitions were observed, sylvite invariably disappeared before the vapour bubble, at temperatures of around 180-220^{o}C and 290-360^{o}C, respectively (Figure 6.4a). The system is therefore undersaturated in KCl. It is also vapour undersaturated, because in the rare instances that the vapour bubble homogenized into the liquid phase with no indication of leakage or decrepitation, it did so at temperatures below the dissolution temperatures of halite and Fe-chloride (430^{o}C to greater than 500^{o}C; Figure 6.4b). Leakage and decrepitation were common from temperatures of about 300^{o}C upwards, but many inclusions which showed no obvious leakage nor decrepitation still contained at least one undissolved daughter at the upper temperature limits of the apparatus (>500^{o}C). A trapping temperature for this fluid is required to constrain isotopic calculations (Section 6.4). In the absence of full homogenization data, a minimum trapping temperature of 500$\pm$100^{o}C is assumed.

Freezing measurements were not obtained, because the small volume and high viscosity of liquid obscured phase changes. The liquid is therefore assumed to be saturated in those salts present as daughters, and its composition estimated using existing solubility data for complex solutions (Section 6.3).

6.2.3 Type II multiphase solid

General characteristics

Inclusions of this type contain a single cubic daughter phase (halite from optical properties), and liquid and gaseous water. They range in size from the lower limit of microscope resolution up to about 5μm, although larger examples were observed (Figure 6.1e). They are relatively uncommon, occurring in discontinuous, planar to irregular arrangements, and are interpreted as pseudosecondary.

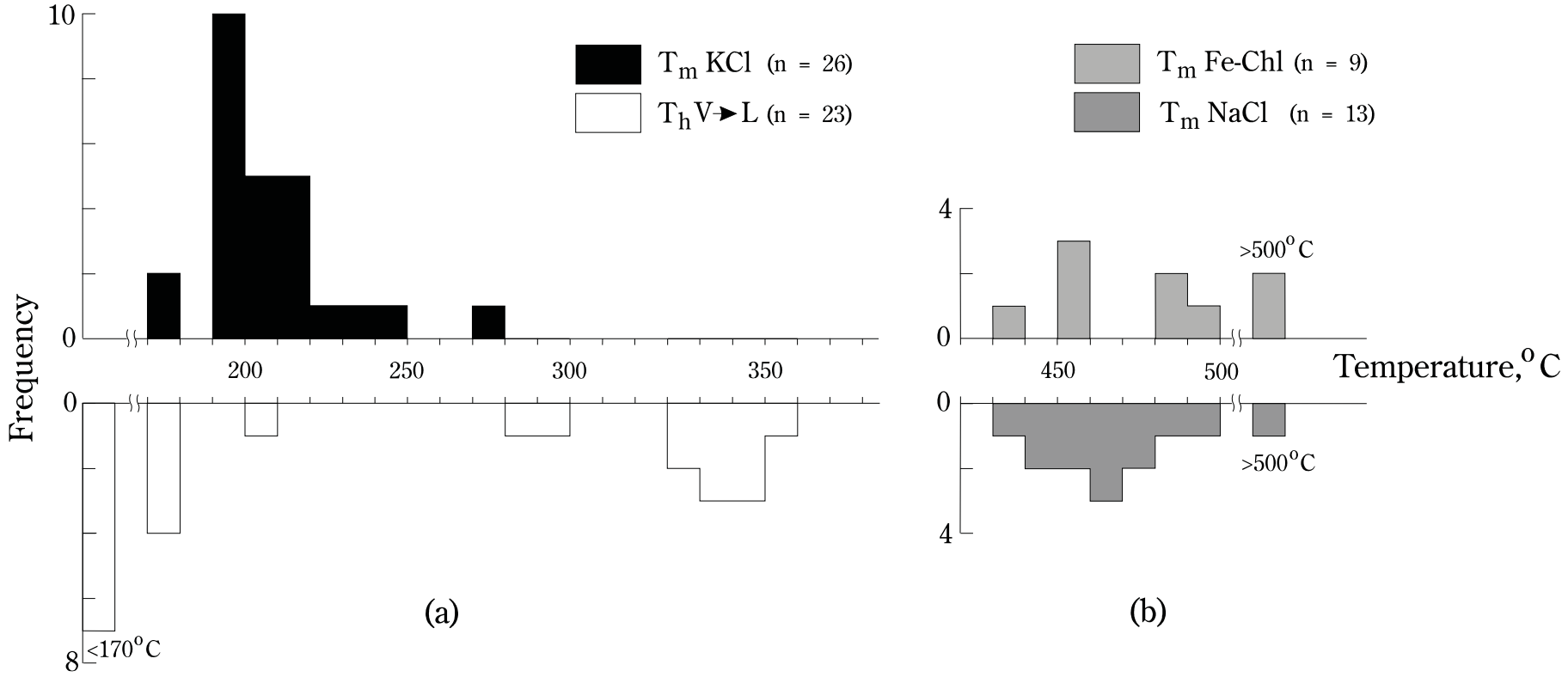

FIGURE 6.4: Thermometric data for Type I multiphase solid inclusions: (a) melting temperature for sylvite (T_mKCl) and temperature of homogenization of vapour into the liquid (T_h V->L), showing that the fluid is undersaturated in KCl; (b)Êmelting temperatures for halite (T_m NaCl) and Fe-chloride (T_m Fe-Chl), showing that these melt at approximately the same temperature, and that the fluid was likely saturated in these components.

Thermometry

No eutectic temperatures were observed for this inclusion population. Final ice melting temperatures were -24 to -25°C (Table 6.4). This is significantly lower than the H_2O-NaCl eutectic temperature, but is close to that for the H_2O-NaCl-KCl system (Table 6.5). Hydrohalite must have been present, but its dissolution temperature was not observed. Vapour homogenized into the liquid phase at temperatures lower than halite dissolution temperatures. Four such inclusions yielded complete homogenization temperatures between 145-190°C, far below those projected for Type I multiphase solid inclusions (*ca.* 500°C). These are minimum trapping temperatures; if the fluid was not salt saturated, the true temperature of trapping will be higher.

Assuming these inclusions contain a simple H_2O-NaCl-KCl fluid, and in the absence of a final dissolution temperature for hydrohalite, thermometric data still constrain the bulk salinity to between about 30 and 33 weight percent, with a maximum of six weight percent KCl, using the experimentally determined phase relations of Sterner *et al.* (1988) for this system (Figure 6.5a). Given the probable presence of Ca^{2+} in other (Type I multiphase solid and Type I liquid-rich two-phase) inclusion populations, the fluid may be better described by the system H_2O-NaCl-$CaCl_2$. Similar bulk salinities are indicated, however, with up to 8 or 9 weight percent $CaCl_2$ (Figure 6.5b).

TABLE 6.4: Thermometric data for Type II multiphase solid fluid inclusions from sample JCU-27163. **T_m(ice)** - final melting temperature of ice; **T_{hL}(vapour)** - homogenization temperature of aqueous liquid and gas phases to liquid; **T_m(halite)** - dissolution temperature of halite.

Inclusion Number	T_m(ice) (°C)	T_{hL}(vapour) (°C)	T_m(halite) (°C)
27163-1			
1	-	118.5±0.5	188±1
3	-24.0±0.1	126.8±0.2	164.5±0.5
4	-25±2	134.5±0.5	145±5
5	-25±2	137.7±0.2	159.5±0.5

TABLE 6.5: Eutectic temperatures for various salt systems. Note particularly that the only common salt in solution which reduces the eutectic temperature to lower than -50°C is $CaCl_2$ (except for $FeCl_3$).

Salt system	**$T_{eutectic}$ (°C)**	**Reference**
H_2O-NaCl	-20.8	Potter *et al.* (1978)
H_2O-KCl	-10.6	Borisenko (1977)
H_2O-$MgCl_2$	-33.6	"
H_2O-$CaCl_2$	-49.5	"
H_2O-$FeCl_2$	-35.0	"
H_2O-$FeCl_3$	-55.0	Linke (1965)
H_2O-NaCl-KCl	-23.5	Borisenko (1977)
H_2O-NaCl-$CaCl_2$	-52.0	Yanatieva (1946)
H_2O-NaCl-$FeCl_2$	-37.0	Borisenko (1977)
H_2O-NaCl-$MgCl_2$	-35.0	"
H_2O-KCl-$CaCl_2$	-50.5	"
H_2O-NaCl-KCl-$CaCl_2$	-55.0	Yanatieva (1946)
H_2O-NaCl-$CaCl_2$-$MgCl_2$	-58.0	Luzhnaya and Vereshtchetina (1946)

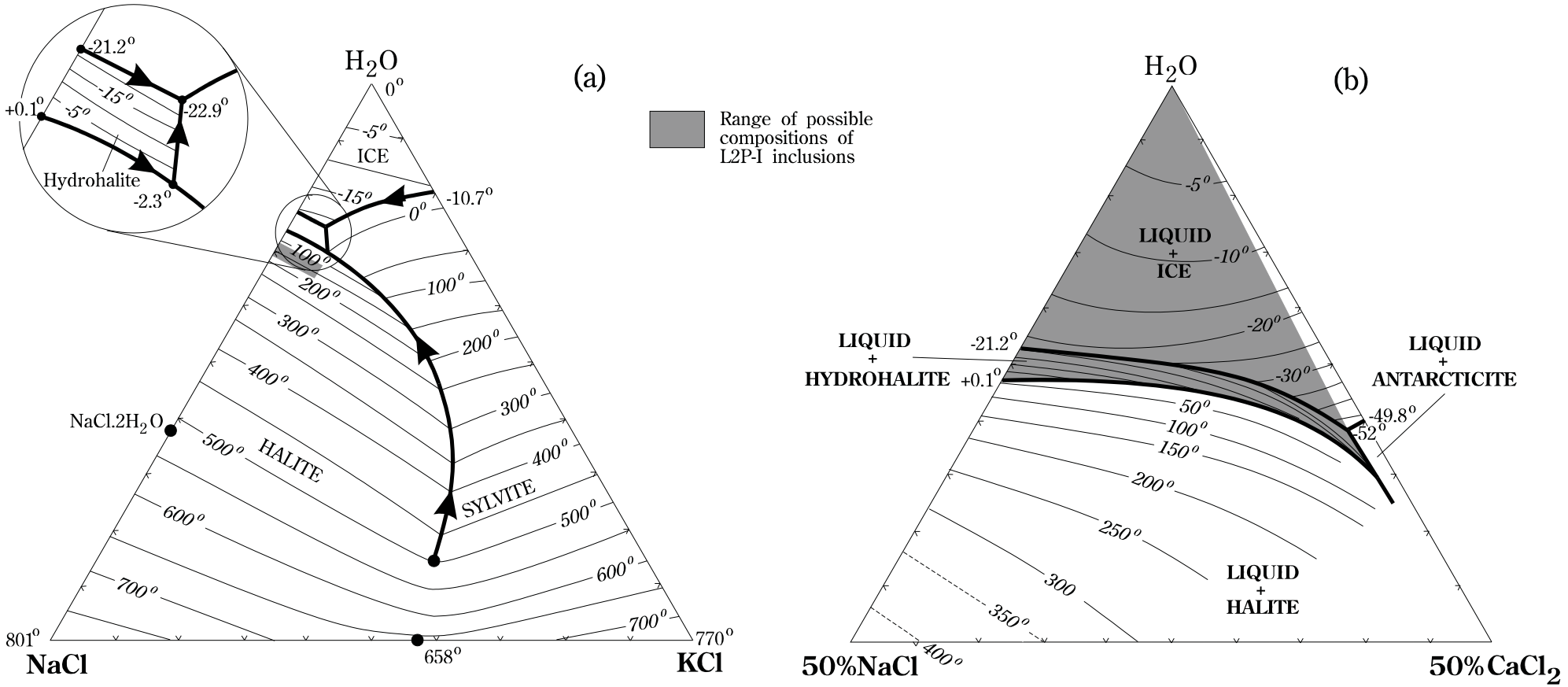

FIGURE 6.5: Temperature-contoured vapour-saturated solubility surfaces in the NaCl-KCl-H_2O and NaCl-$CaCl_2$-H_2O systems. The shaded areas represent the estimated ranges of possible compositions for Type II multiphase solid inclusions, assuming the fluid belongs to one or other of the systems. Note that in either case, a maximum solubility of about 30wt% total dissolved salt is implied. (a) is after Figure 3 of Sterner *et al.* (1988); (b) is after Figure 1 of Williams-Jones and Samson (1990).

6.2.4 Immiscible liquid

General characteristics

These are characterized by the coexistence of liquid and gaseous CO_2, and the occasional presence also of an aqueous liquid. CO_2 was identified by its greyer appearance relative to the aqueous phase, the rapid "jiggling" of the gaseous CO_2 bubble within the liquid CO_2, by the homogenisation of liquid and gaseous CO_2 to a single phase at temperatures less than 31^{o}C, and by its melting temperature. The proportion of aqueous liquid varies from inclusion to inclusion. CO_2-bearing inclusions are more common in some samples than is apparent at first glance, as several inclusions which were initially interpreted as aqueous liquid- or vapour-only inclusions nucleated a gaseous CO_2 phase at the initiation of some cooling runs, indicating that these inclusions actually contained CO_2.

Immiscible liquid inclusions occur aggregated into irregular pseudosecondary planes, or as isolated individuals of primary appearance (Figures 6.1f), spatially associated with Type I multiphase solid inclusions. Rare variants of this type of inclusion contain CO_2 in the liquid and vapour phase and solids in the aqueous phase (Figure 6.1g).

Thermometry

Six examples were studied thermometrically from a sample also containing abundant other inclusion types (JCU-27163; Table 6.6). During cooling runs, final -melting temperatures were within a few tenths of a degree of the melting temperature for pure CO_2 (-56.6^{o}C). The slightly low measured melting temperature may be due to imprecision in measurement, or to the presence of minor amounts of another gaseous phase such as CH_4. Clathrate melting temperatures in H_2O-bearing examples were not observed.

During heating runs, all liquid and vapour CO_2 homogenized to the liquid phase, at temperatures less than the critical temperature for pure CO_2 (31.1°C). The proportion of H_2O coexisting in CO_2-bearing inclusions at this time approaches 50 percent in some instances, but CO_2 is dominant in the majority of such inclusions (generally close to 100 percent). CO_2-bearing inclusions decrepitated from temperatures around 300°C, before complete homogenization of H_2O-bearing examples to a single fluid phase.

TABLE 6.6: Thermometric and volumetric data for CO_2-bearing fluid inclusions from sample JCU-27163. **$T_m(CO_2)$** - final melting temperature of solid CO_2; **$T_{hL}(CO_2)$** - homogenization temperature of CO_2 liquid and gas phases to liquid CO_2; **CO_2:H_2O (31°C)** - ratio of CO_2 to water after CO_2 homogenization; **T_d** - decrepitation temperature of inclusion. Hyphen - transition occurred, but the temperature not recorded. Homogenization of CO_2-H_2O-bearing inclusions to a single phase did not occurred before decrepitation.

Inclusion Number	$T_m(CO_2)$ (°C)	$T_{hL}(CO_2)$ (°C)	CO_2:H_2O (31°C)	T_d (°C)
1	-56.75±0.05	30.15±0.05	0.5	310
2	-	21.05±0.05	0.55	-
8	-56.95±0.05	27.45±0.1	0.99	-
10	-56.95±0.05	26.15±0.05	1.00	-
13	-	6.0±0.05	1.0	-
14	-	12.1±0.1	1.0	-

6.2.5 Type I liquid-rich, two-phase inclusions

General characteristics

These amorphous to crudely regular inclusions occur in pseudosecondary planes scattered through the host quartz. Some of these planes cut across the earlier highly saline primary inclusions. Individual inclusions are aqueous, and have a high degree of fill (generally greater than 0.95). Liquid-rich two-phase inclusions with a similar degree of fill are present rarely in carbonate. These are highly elongate along crystallographic planes, and bearing in mind the fact that carbonate formed later than quartz, may be primary or pseudosecondary (Figure 6.1h,i).

Thermometry

First melting was interpreted as occurring at the first appearance of granularity and darkening (by dispersion of light) in the ice. Slight movement of the vapour bubble was observed in rare instances. These changes were difficult to pick, and eutectic temperatures were consequently only rarely measured precisely, instead being constrained as maximums. The data show a cluster between about -40 and -46^{o}C, and another from -50 and -59^{o}C (Figure 6.6a), but accurately measured eutectic temperatures were generally less than -50^{o}C, and the bimodal distribution may not be significant.

Table 6.5 summarizes eutectic temperatures for a number of relatively simple water-salt systems, and it is clear that temperatures significantly lower than -40^{o}C require a solution of several salt species, at least one of which must be divalent. One or all of Ca^{2+}, Mg^{2+} and Fe^{2+} could account for the observed eutectic temperatures, since all have been identified from an earlier stage in the history of fluid evolution (preserved in Type I multiphase solid inclusions).

Final ice melting temperatures range from between about -25 and 0^{o}C, sometimes within a single sample (*e.g.* JCU-27163). Hydrohalite must have been present, but it could not be detected amongst the more abundant, higher relief ice. Figure 6.6b suggests that there are several populations, but this is an artefact deriving from the small data set, and the fact that some samples (*e.g.* JCU-27273 and 27262) provided data from several inclusions belonging to a single generation. Results are therefore biased towards concentrations of particular temperatures. With further sampling, a continuous range of final ice melting temperatures is expected.

Fluids trapped in these inclusions should properly be ascribed to the system NaCl-KCl-$CaCl_2$-$FeCl_2$-$MgCl_2$ (at least), but the phase relations for this system are unknown. A simpler system consistent with the low-temperature thermometric data, and for which some phase relation data exist is H_2O-NaCl-$CaCl_2$ (Figure 6.5b). Unfortunately, without hydrohalite melting temperatures the points at which the liquid

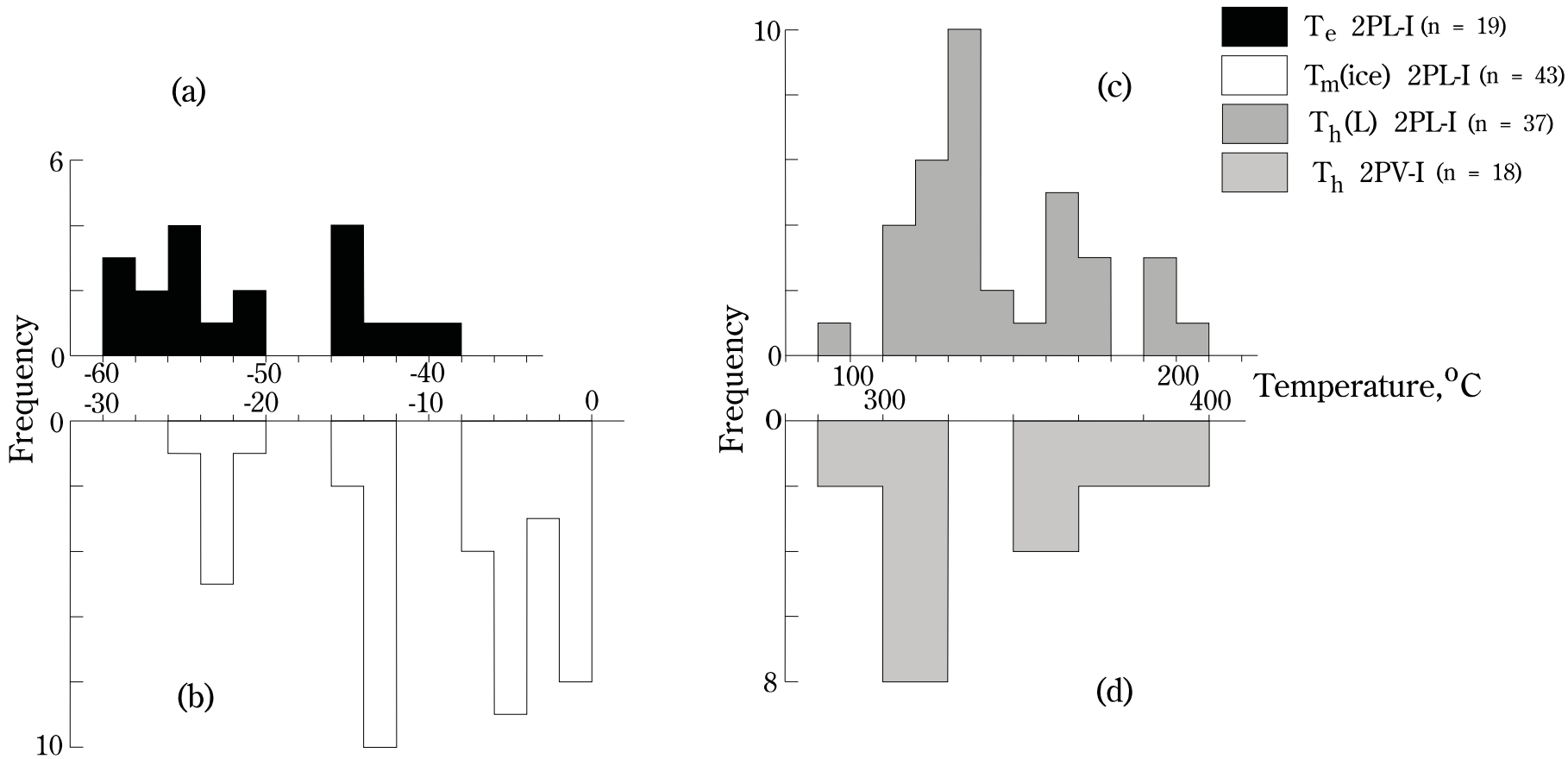

FIGURE 6.6: Thermometric data for Type I liquid-rich two-phase inclusions: (a) eutectic (first-melting) temperatures (T_e 2PL-I); (b) final ice-melting temperature (T_m(ice)); (c) uncorrected (for pressure) temperatures of homogenization of vapour into the liquid (T_h(L)); (d) uncorrected (for pressure) temperatures of homogenization for vapour-rich, two-phase inclusions, usually to liquid (T_h 2PV-I).

compositions leave the ice-hydrohalite cotectic cannot be located, and the bulk liquid salinity cannot be constrained more accurately than being somewhere in the salt-undersaturated ice+liquid field, or less than about 25 weight percent total dissolved salt. If the fluid is related to that preserved in Type II multiphase solid inclusions, the $CaCl_2$ content may be restricted to less than about 10 weight percent. Ice melting temperatures close to 0^oC suggest a fluid approaching pure water in composition.

Uncorrected homogenization temperatures were generally less than about 200^oC (Figure 6.6c). The data are crudely bimodal for the same reasons as the ice-melting data, but there is an ill-defined tendency for lower final ice melting temperatures to correlate with lower final homogenization temperatures. "Pressure corrections" to the homogenization temperatures are required to determine the temperature of vapour saturation (boiling), and hence the maximum trapping temperature, at the confining pressure prevailing at the time of trapping.

Liquid-vapour phase relations for salt solutions are only known in any detail for the system H_2O-NaCl, and the pressure correction calibrations of Potter (1977) for this system are used here as an approximation. The maximum possible confining pressure is constrained by contact metamorphic assemblages to less than 200-250 MPa, which yields a maximum temperature correction for salinities up to about 25 weight percent NaCl of less than 200^oC. Brittle processes occurring during contemporaneous faulting suggests that confining pressures were probably significantly lower, perhaps less than 100 MPa, requiring a correction of less than 100^oC. Maximum corrected homogenization temperatures are therefore only up to 300 or 400^oC (for 100 and 200 MPa, respectively), which are still significantly lower than those for primary Type I multiphase solid inclusions. If fluid pressure was abruptly lowered from lithostatic to near hydrostatic during fault rupture, corrections would be of even smaller magnitude.

6.2.6 Type II liquid-rich, two-phase inclusions

General characteristics

These secondary inclusions are very abundant, occurring in planes which transect all other groups of fluid inclusion types, and which are commonly so closely packed as to obscure or destroy earlier inclusion features of the host (*e.g.* Figure 6.1-l). The inclusions are generally small (less than 2 μm) and aqueous. Liquid/vapour ratios are difficult to resolve, but may be variable.

Thermometry

None of the secondary inclusions were large enough to study systematically, although some examples were observed to have homogenized at (uncorrected) temperatures lower than for other inclusion types. They are assumed to represent very late stage, relatively dilute, cool fluids introduced well after the alteration and mineralizing events.

6.2.7 Vapour-rich, two-phase inclusions

General characteristics

Vapour-enriched inclusions are commonly spatially associated with Type II multiphase solid and Type I liquid-rich, two phase inclusions. They appear to be exclusively aqueous, with a variable degree of fill (≤ 0.6), and sizes ranging up to 10 μm (*e.g.* Figure 6.1l).

Thermometry

Apart from a single eutectic temperature of -45°C, no subzero phase changes were recorded. The salinity of the fluid in these inclusion is therefore unknown.

Homogenization usually occurred to the liquid phase, at temperatures of 200 to 400°C (Figure 6.6d). There was a trend for vapour-rich inclusions with lower degrees of fill to homogenize at progressively higher temperatures, which suggests their formation by post-entrapment necking of inclusions rather than by boiling.

6.2.8 Solid inclusions

General characteristics

Solid inclusions of a cubic phase up to 5 μm in diameter were observed in rare instances, spatially associated with Type I and II multiphase solid and vapour-rich two phase inclusions (*e.g.* Figures 6.1m,n). Their presence is revealed by thin films of liquid, sometimes containing small vapour bubbles, around at least parts of their rims. Where liquid is absent the contacts with the quartz host rims are near invisible, indicating a similar refractive index. The solid inclusions are interpreted to be halite. The density of packing, and the absence of related liquid- or vapor-rich "co-necked" inclusions suggest that they may have originally been present as solids supported in the (highly saline) primary fluid, rather than due to post-entrapment necking of ordinary primary fluid inclusions.

6.2.9 Spatial and temporal relations between inclusion populations

Useful fluid inclusions are comparatively uncommon in the quartz host, because they are preserved only in vein and vugh infill; most quartz occurs as replacement. Where specimens contain useable inclusions, examples of several populations are usually present. Most examined infill quartz has a "dusty" appearance arising from the profusion of very small secondary inclusions in bands of closely-spaced planes. Where most densely developed, it was difficult to resolve individual planes. "Clean" areas with few secondary inclusion planes are sparse (*e.g.* Figures 6.1h,k), and it is only in these regions where primary Type I and II multiphase solid

inclusions are preserved. These inclusions are therefore amongst the rarest types. The primary and pseudosecondary inclusions used in this study are only those which are greater than at least several primary inclusion diameters from the nearest obvious secondary inclusion planes, and which show no other evidence of modification by secondary fluids.

CO_2-bearing (immiscible fluid) inclusions are extremely rare, and where observed are most closely associated with Type I multiphase solid inclusions. The latter are only rarely spatially associated with aqueous vapour-rich inclusions, however, and the vapour phase in the former homogenizes to liquid before the dissolution of the daughters. Vapour undersaturated conditions therefore generally prevailed during trapping; the early fluid was not boiling, and the rare instances where an association is observed are probably coincidental.

Vapour-rich inclusions are most commonly spatially associated with Type II multiphase solid (halite only) and Type I liquid-rich two-phase inclusions. Liquid-rich inclusions are the most abundant of the relatively large (>5 μm) inclusions. Despite this association, there is no unequivocal evidence for boiling; vapour-rich inclusions homogenize at temperatures different from all other inclusion types. Some Type I liquid-rich two-phase inclusions show phase changes (final ice melting and vapour disappearance) at similar temperatures to the same changes in Type II multiphase solid inclusions. This suggests the former may have bulk compositions differing only in being NaCl undersaturated at room temperature, and that the two populations may be close to coeval.

The temporal relationship between halite solid inclusions and other inclusion types is uncertain. They were only rarely observed (*e.g.* Sample JCU-27096 I #1), and are spatially associated with, and of a similar size to both Type I and Type II multiphase solid inclusions. Their presence indicates NaCl oversaturation of the fluid, and they may have been carried in suspension in the most highly saline, viscous fluid (*i.e.* Type I).

The overall trend in fluid characteristics represented by the sequence of primary to pseudosecondary to secondary inclusions is one of decreasing temperature and salinity. Early inclusions trapped a highly saline fluid at high temperature; later inclusions trapped salt-undersaturated fluid at lower temperature. This trend indicates fluid dilution, and places important constraints on modelling of fluid evolution, as boiling cannot explain this trend (see Discussion - Sections 6.5.2 and 6.5.4).

6.3 VOLUMETRIC STUDIES

6.3.1 Introduction

Semi-quantitative estimates of near-primary fluid composition were obtained by measuring the volumes of liquid, vapour and daughter phases in twenty-eight primary Type I multiphase solid inclusions. The details of this technique are recorded in Appendix C. Daughters were identified using optical properties and semi-quantitative SEM analyses. Published salt solubility data have been used to approximate the overall fluid chemistry of the homogeneous fluid (*i.e.* at the time of trapping). The technique assumes that:

(i) fluid trapped in inclusions was homogeneous and representative of the bulk of the fluid at the time;

(ii) fluid inclusions have remained closed systems since trapping, irrespective of whether they are primary or not; and

(iii) major daughter minerals precipitated from the fluid at or after trapping, and do not represent extraneous inclusions.

Inclusions are trapped at the surface of a growing crystal, where "boundary layer" compositional gradients are likely to be most pronounced. Roedder (1984, p. 39) has argued that the width of this boundary layer will have negligible effect on the bulk composition of trapped fluid under geological conditions, because diffusion is rapid compared to crystal growth rates, particularly where large inclusions (greater than 5-10 μm) are considered.

That inclusions have remained closed to all components is more difficult to substantiate. Those used showed no evidence of necking, nor of bulk leakage by decrepitation or fracturing. Minor volume changes might be expected through precipitation of host material originally in solution, but these are probably negligible. The effects of diffusion of components from the system could not be assessed. H_2 is the most likely component to escape in this manner, but laser-Raman spectroscopic studies of inclusions in quartz from a number of different environments have detected H_2, suggesting that leakage via diffusion is not significant (Shepherd *et al.*, 1985, p.13).

Haematite flakes occurring inconsistently in Type I multiphase solid inclusions could represent irreversible precipitation through oxidation of Fe^{2+} in the fluid by diffusion of H_2 from the inclusion, as suggested by Roedder and Skinner (1968). Haematite was, however, being precipitated in association with quartz veining as part of the alteration paragenesis at the time of fluid inclusion formation (Chapter 5), indicating that the fluid was relatively oxidized (above the haematite-magnetite buffer). H_2 diffusion is therefore not required and, if haematite flakes do not represent true daughter phases, accidental trapping of haematite inclusions is the preferred mechanism of preservation. The $CaCl_2$-bearing fluid existing at the time (Section 6.3.3) is likely to have been very viscous (Potter and Clynne, 1978), and capable of entraining solid phases.

The consistency in the relative number, identity and volume proportion of major trapped solids supports the interpretation that they are true daughter phases.

6.3.2 Solution composition at room temperature

The composition of the homogeneous fluid originally trapped in Type I multiphase solid inclusions is calculated from the amount of solute contained in the solid phases and the composition of the coexisting liquid phase at room temperature. The amount of material contained in the daughter phases is reasonably well-constrained, given their known compositions and regular, easily measured crystal

shapes. The liquid composition is the least well-constrained, because the irregular shapes of the inclusions yield large inaccuracies in volumetric measurements, and because experimental data on complex chloride solutions is almost non-existent.

Halite, sylvite, antarcticite, $FeCl_2.2H_2O$, calcite, dolomite and haematite are confirmed daughters in these inclusions. The coexisting liquid must therefore be saturated in those phases. Such a system is far more complicated than those for which experimental data exist, and several simplifying assumptions must be applied.

Mg-chloride species were not observed in the daughter assemblage, and calcite and dolomite, although commonly present, are volumetrically insignificant, contributing little to the cation content of the coexisting liquid. The contribution of Ca^{2+} to the system by carbonate is calculated assuming all carbonate is calcite, and the Mg content in the liquid is (probably invalidly) assumed to be negligible.

Haematite is also negligible volumetrically, and its contribution to the overall amount of Fe^{3+} in solution is neglected. Its significance for the oxidation state of the fluid is important, however (see Section 6.5).

Eutectic temperatures determined from pseudosecondary Type I liquid-rich two-phase inclusions suggest the presence of dissolved Ca^{2+} (Section 6.2.5). The (rare) occurrence of antarcticite suggests that the liquid in at least some of the studied Type I multiphase solid inclusions is saturated in $CaCl_2$. $CaCl_2$ is a highly soluble salt, and must be present in considerable quantities to produce a saturated fluid. The liquid is assumed to be saturated with respect to $CaCl_2$, whether antarcticite is present or not.

The simplest system which describes the liquid in the inclusions used is therefore NaCl-KCl-$CaCl_2$-$FeCl_2$-H_2O. Experimental solubility data for the complete system are lacking, but may be estimated using data from subsets of this system, and empirical observations. A solution coexisting with sylvite, halite and antarcticite at 25^{o}C contains KCl, NaCl and $CaCl_2$ in the weight percent ratio of 3.2:0.6:44.8 (after Yanatieva in Linke, 1965, p.587). The solubility of Fe^{2+} in a solution also saturated in

KCl, NaCl and $CaCl_2$ has not been determined, and must be estimated indirectly using existing experimental data on the $CaCl_2$-KCl-NaCl-H_2O system and an approximation of Fe concentration in solution.

Transport of iron in chloride-rich solutions at geological temperatures is predominantly as an associated chloride complex, and the dominant Fe-bearing species in solution in equilibrium with haematite (at 400-600^oC and 100 and 200 MPa) is $FeCl_2^o$ (Chou and Eugster, 1977; Boctor *et al.*, 1980). Few data exist, however, for the amount of iron dissolved in these brines. Naumov and Shapenko (1980) performed some empirical analyses on highly saline fluid inclusions from the Tyrnyauz skarn deposit in the North Caucasus. They concluded that for fluid inclusions containing sodium and potassium chlorides, in addition to iron-bearing solid phases, the initially homogeneous chloride solutions at 400-700^oC contained 1-7 wt% of iron (presumably as Fe^{2+}).

Kwak *et al.* (1986) estimated iron solubility at less than 3 weight percent in a liquid also containing $CaCl_2$, NaCl and KCl at 25^oC, using the known solubilities of cations with similar geochemical properties, such as $MgCl_2$ and $CoCl_2$. Wood (1975) calculated solution compositions in equilibrium with various invariant mineral assemblages in the NaCl-KCl-$MgCl_2$-$CaCl_2$-H_2O system at 25^oC, finding that they agreed reasonably well with experimentally determined solubility data. His results are presented in Table 6.7 as weight percent solute species in solution. It is apparent that solutions in equilibrium with solid assemblages of Na-, Ca- and Mg-salts, or K-, Ca- and Mg-salts contain between 12 and 17wt% $MgCl_2$ in solution. In the four-salt system, all phases would probably be somewhat less soluble.

These data suggest that in the NaCl-KCl-$CaCl_2$-$FeCl_2$-H_2O system, a fluid in equilibrium with these salts at 25^oC might contain about 10 weight percent $FeCl_2$ in solution. The liquid composition used in compositional calculations based on the volumetric studies is therefore taken as:

$CaCl_2$ 44.82wt% : KCl 3.22wt% : NaCl 0.62wt% : $FeCl_2$ 10.0wt% : H_2O 31.34wt%

TABLE 6.7: Calculated solution compositions (wt%) and H_2O activities in equilibium with various invariant mineral assemblages in the system NaCl-KCl-$MgCl_2$-$CaCl_2$-H_2O at 25°C. Adapted from Table 6 (p.1155) of Wood (1975).

Abbreviations for solid phases:

at	antarcticite	($CaCl_2.6H_2O$)	**n**	halite	(NaCl)
bi	bischoffite	($MgCl_2.6H_2O$)	**sy**	sylvite	(KCl)
c	carnallite	($KMgCl_3.6H_2O$)	**ta**	tachyhydrite	($CaMg_2Cl_6.12H_2O$)

Assemblage	**aH_2O**	**wt% NaCl**	**wt% KCl**	**wt% $MgCl_2$**	**wt% $CaCl_2$**	**wt% Cl^-**
n + sy + soln	0.726	20.39	11.22	-	-	17.70
n + sy + c + soln	0.568	3.59	4.73	25.74	-	21.36
n + bi + c + soln	0.366	0.567	0.114	34.43	-	27.14
n + bi + soln	0.376	0.591	-	38.10	-	28.0
n + bi + ta + soln	0.243	0.083	-	12.27	31.18	32.76
n + bi + at + soln	0.281	0.125	-	13.68	27.02	33.08
n + ta + at + soln	0.281	0.116	-	16.67	21.76	35.58
n + at + soln	0.413	0.33	-	-	37.08	32.16
at + ta + soln	0.224	-	-	11.94	34.25	30.74
bi + ta + soln	0.232	-	-	14.59	30.73	30.46
sy + at + soln	0.353	-	0.66	-	41.53	29.39
sy + at + ta + soln	0.248	-	0.421	14.06	28.65	32.52
sy + ta + bi + soln	0.242	-	0.393	12.30	31.02	32.72

The density of the liquid is required for mass calculations. Naumov and Shapenko (1980) calculated the density of saline brines from fluid inclusions containing Fe-chloride daughters at 1.5 $\pm$ 0.2 g.cm^{-3}. Yanatieva (1946) reported that a saturated liquid in the $CaCl_2$-NaCl-KCl-H_2O system has a density of 1.469 g.cm^{-3}. A density of 1.5 g.cm^{-3} is used in the geochemical calculations.

6.3.3 Homogeneous fluid composition

Complete volumetric data and results of fluid composition calculations are recorded in Appendix F2, and summarized in Tables 6.8 through 6.10. Volumes of solid halite, sylvite and Fe-chloride are dominant over antarcticite and carbonate in Type I multiphase solid inclusions at room temperature (Table 6.8). This does not necessarily imply dominance of these phases in the original homogeneous solution, however, because an inclusion containing a fluid and coexisting halite, sylvite, Fe-chloride and antarcticite will have most NaCl and KCl in the solid phases, and most $CaCl_2$ in the liquid phase (Section 6.3.2). Calculated compositions of major species in the original homogeneous fluid are presented in Table 6.9. Ratios of major cationic species are compiled in Table 6.10. This fluid is a highly saline chloride brine having an average of 73.7 weight percent total dissolved salt. NaCl is very high (average 26.24 weight percent), as may be expected, but so too is $CaCl_2$ (average 27.62 weight percent). The latter may be overestimated as a result of initial assumptions about solution composition at room temperature. KCl and $FeCl_2$ contents are subordinate (average 9.34 and 9.45 weight percent, respectively).

$CaCl_2$ and $FeCl_2$ contents are less variable than those of NaCl and KCl. This again relates to the assumption that $CaCl_2$ and $FeCl_2$ are largely in solution at room temperature, and that NaCl and KCl are predominantly in halite and sylvite, with little in solution. Calculated abundances of the first two therefore depend largely on initial assumptions about concentrations of these species in solution (assumed constant), whereas calculated abundances for NaCl and KCl are subject to systematic errors in daughter and inclusion volume measurement, and therefore inherently prone to greater variation. This fluid is unlikely to represent the true primary fluid composition, the probable composition of which is considered below (Section 6.5.1).

TABLE 6.8: Volume percentages of all phases in fluid inclusions used for volumetric studies.

SAMPLE	vol% NaCl	vol% KCl	vol% $FeCl_2.2H_2O$	vol% Fe_2O_3	vol% $CaCl_2.6H_2O$	vol% $CaCO_3$	vol% liquid	vol% vapour
27068-4	20.0	14.1	1.9	-	0.3	0.4	59.2	4.1
27086-1	19.6	15.1	6.7	-	-	1.3	55.0	2.1
27086-5	20.9	3.2	6.1	-	-	0.2	67.8	1.7
27086-9	32.2	9.8	5.4	-	-	0.6	47.6	4.3
27086-10	14.1	0.5	3.7	-	-	1.2	77.1	3.4
27086-11[1]	53.2	3.8	6.6	-	-	0.1	34.8	1.5
27094-1	11.1	8.5	4.8	-	0.5	0.8	73.5	0.8
27094-7	17.2	7.4	1.6	-	0.8	2.5	69.5	1.0
27094-10	23.4	2.9	2.9	-	0.4	1.0	68.9	0.5
27094-11	15.7	12.1	7.4	-	-	2.2	56.7	5.9
27094-12	20.9	7.7	2.8	-	0.04	0.8	66.3	1.5
27110-1	11.9	2.1	1.9	-	-	0.1	81.4	2.6
27110-2	26.9	3.4	2.6	-	-	0.7	62.6	3.8
27110-3	27.2	2.4	3.9	-	-	0.3	59.9	6.3
27110-4	22.0	4.6	3.2	-	-	0.8	60.9	8.1
27199-1	16.4	4.5	1.5	-	-	0.5	75.4	1.7
27199-2	15.9	6.2	2.4	-	-	-	72.7	2.7
27199-3	19.0	5.2	1.5	-	-	-	70.2	4.1
27199-6	12.2	2.6	1.3	-	-	-	80.2	3.7
27199-9	28.0	5.7	0.5	-	-	-	64.0	1.8
27271-1	17.4	3.8	1.5	-	-	-	74.9	2.5
27271-4	29.2	4.3	3.5	-	-	0.3	59.8	2.9
27271-9	17.7	3.3	2.0	-	-	-	72.3	4.7
27273-1	26.5	9.1	4.7	0.01	0.3	0.4	50.4	8.6
27273-4	13.2	3.9	2.0	-	0.1	0.4	74.4	6.1
27273-5	11.7	2.5	3.6	0.00001	0.45	0.5	68.5	12.0
27273-8	12.8	4.3	0.2	-	-	2.5	70.2	9.7
27273-10	20.5	6.5	1.0	-	-	0.3	63.5	8.1
AVERAGE	19.39	5.77	2.99	-[2]	0.36[3]	0.85[4]	66.77	4.25
σ	5.84	8.51	3.62	-	0.22	0.71	8.5	2.91

[1] This sample is anomalous, and not included in the calculations of average and standard deviation.

[2] Average and standard deviation for the two existing measurements of Fe_2O_3 is pointless.

[3] Average of the eight existing measurements of antarcticite.

[4] Average of the twenty-one acceptable measurements of $CaCO_3$.

TABLE 6.9: Calculated composition of the homogeneneous hydrothermal fluid trapped in Type I multiphase solid inclusions, in terms of weight percent dissolved salts (NaCl, KCl, $FeCl_2$, $CaCl_2$ and $CaCO_3$), as molarities (**M** = mole of solute per litre of solution), and as molalities (**m** = mole of solute per kilogram of solvent; H_2O in this case). Means and standard deviations for concentrations of NaCl, KCl, $FeCl_2$, $CaCl_2$ and Cl^- are calculated using 27 of the 28 anlayses; 27086-11 is excluded because it is clearly anomalous. Mean and standard deviation for "calcite" are calculated using the 21 existing wt% values. Calcite is assumed to have negligible solubility at room temperature, and its weight percent in inclusions is therefore that determined for the solid daughter phase.

SAMPLE	NaCl wt%	M Na^+	m Na^+	KCl wt%	M K^+	m K^+	$FeCl_2$ wt%	M Fe^{2+}	m Fe^{2+}	$CaCl_2$ wt%	$CaCO_3$ wt%	M Ca^{2+}	m Ca^{2+}	Cl^- wt%	M Cl^-	m Cl^-	total wt% salt	H_2O wt%
27068-4	26.46	7.543	19.887	18.55	4.14	10.915	7.48	0.982	2.588	24.03	0.7	3.722	9.814	44.41	20.885	55.063	77.22	22.78
27086-1	24.66	7.365	19.566	18.71	4.383	11.643	11.85	1.631	4.334	21.17	2.06	3.683	9.783	44.04	20.514	54.497	78.45	21.55
27086-5	27.29	7.873	17.382	5.75	1.298	2.867	12.8	1.698	3.749	27.09	0.17	4.136	9.132	43.75	19.329	42.676	73.1	26.9
27086-9	38.54	11.994	37.011	11.95	2.921	9.014	9.46	1.361	4.201	21.3	0.97	3.061	9.446	45.57	23.473	72.433	82.22	17.78
27086-10	30.18	9.465	19.009	2.55	0.626	1.257	10.08	1.461	2.935	28.25	1.82	4.99	10.022	43.21	22.376	44.938	72.87	27.13
27086-11	60.28	19.805	79.107	4.87	1.253	5.005	9.1	1.379	5.508	12.17	0.2	2.142	8.557	51.75	28.055	112.061	86.96	13.04
27094-1	14.89	4.223	8.689	12.37	2.755	5.667	12.08	1.583	3.256	30.08	1.26	4.708	9.687	40.89	19.139	39.377	70.69	29.31
27094-7	22.56	6.505	14.572	10.72	2.425	5.433	8	1.059	2.373	28.16	4.05	4.953	11.096	41.25	19.608	43.925	73.49	26.51
27094-10	30.32	8.792	19.51	5.39	1.226	2.72	9.25	1.237	2.744	27.82	0.64	4.351	9.655	43.9	20.942	46.473	73.42	26.58
27094-11	20.74	5.924	15.158	16.07	3.601	9.213	13.35	1.759	4.502	22.84	3.58	4.035	10.323	42.28	19.918	50.964	76.59	23.41
27094-12	27.13	7.85	18.42	11	2.495	5.854	8.94	1.194	2.801	26.38	1.34	4.265	10.009	43.55	20.789	48.784	74.8	25.2
27110-1	16.9	4.541	8.822	5.21	1.096	2.129	10.07	1.246	2.421	34.86	0.15	4.952	9.621	40.63	18.055	35.079	67.23	32.77
27110-2	35.3	10.089	25.092	5.81	1.302	3.237	8.56	1.129	2.809	25.2	1.04	3.965	9.861	45.07	21.175	52.662	75.92	24.08
27110-3	36.37	10.191	25.991	4.7	1.034	2.638	9.92	1.282	3.27	24.6	0.46	3.719	9.486	45.56	21.046	53.679	76.05	23.95
27110-4	26.9	8.314	20.978	18.81	4.541	11.459	8.41	1.192	3.008	22.76	1.19	3.906	9.856	44.5	22.588	56.996	78.06	21.94
27199-1	22.24	6.193	13.013	7.73	1.69	3.552	8.68	1.114	2.34	31.2	0.88	4.717	9.912	41.96	19.296	40.55	70.74	29.26
27199-2	21.8	6.038	13.032	9.83	2.13	4.597	9.46	1.208	2.606	30.24	-	4.405	9.508	42.51	19.399	41.87	71.34	28.66
27199-3	26.14	7.186	16.217	8.55	1.842	4.156	8.25	1.043	2.353	29.43	-	4.267	9.629	43.34	19.602	44.234	72.38	27.62
27199-6	17.53	4.661	9.247	5.89	1.225	2.431	9.33	1.141	2.263	34.76	-	4.86	9.643	40.85	17.865	35.447	67.5	32.5
27199-9	36.22	10.483	26.233	8.52	1.937	4.846	6.2	0.829	2.075	25.44	-	3.873	9.692	45.75	21.927	54.868	76.39	23.61
27271-1	23.87	6.579	13.937	6.89	1.504	3.186	8.68	1.104	2.338	31.25	-	4.538	9.614	42.58	19.334	40.958	70.69	29.31
27271-4	37.4	10.935	28.12	6.74	1.545	3.973	9.03	1.218	3.132	23.53	0.52	3.712	9.545	45.98	22.071	56.757	77.22	22.78
27271-9	24.71	6.697	14.596	6.36	1.347	2.935	9.24	1.153	2.514	30.69	-	4.383	9.553	42.8	19.099	41.626	71.01	28.99
27273-1	35.34	9.913	29.174	12.51	2.759	8.121	9.9	1.28	3.767	20.84	0.66	3.143	9.249	46.24	21.385	62.935	79.27	20.73
27273-4	19.01	5.009	10.606	7.37	1.523	3.224	9.64	1.17	2.477	32.53	0.75	4.627	9.797	41.22	17.874	37.842	69.31	30.69
27273-5	18.09	4.45	9.951	5.81	1.119	2.503	11.78	1.336	2.987	32.27	0.95	4.315	9.648	40.94	16.61	37.139	68.91	31.09
27273-8	19.02	4.855	11.118	8.05	1.611	3.688	7.36	0.866	1.984	31.67	4.6	4.913	11.251	39.72	16.686	38.213	70.7	29.3
27273-10	28.93	7.733	19.366	10.28	2.157	5.401	7.31	0.901	2.256	27.36	0.56	3.932	9.847	44	19.421	48.638	74.43	25.57
Average	26.24	7.46	17.95	9.34	2.08	5.06	9.45	1.23	2.89	27.62	1.35	4.23	9.8	43.2	20.02	47.36	73.7	26.3
σ	6.77	2.16	6.96	4.39	1.05	2.96	1.68	0.23	0.68	4.05	1.21	0.52	0.45	1.82	1.71	8.9	3.71	3.71

TABLE 6.10: Ratios of major cationic species identified in fluid inclusions used for volumetric studies.

SAMPLE	molar K^+/Na^+	molar Ca^{2+}/Na^+	molar Fe^{2+}/Na^+
27068-4	0.55	0.494	0.13
27086-1	0.595	0.5	0.222
27086-5	0.165	0.525	0.216
27086-9	0.244	0.255	0.114
27086-10	0.066	0.527	0.154
27086-11	0.063	0.108	0.07
27094-1	0.652	1.115	0.375
27094-7	0.373	0.761	0.163
27094-10	0.139	0.495	0.141
27094-11[1]	0.607	0.681	0.297
27094-12	0.318	0.543	0.152
27110-1	0.241	1.091	0.274
27110-2	0.129	0.393	0.112
27110-3	0.102	0.365	0.126
27110-4	0.546	0.47	0.143
27199-1	0.273	0.762	0.18
27199-2	0.353	0.73	0.2
27199-3	0.256	0.594	0.145
27199-6	0.263	1.043	0.245
27199-9	0.185	0.37	0.079
27271-1	0.229	0.69	0.168
27271-4	0.141	0.339	0.111
27271-9	0.201	0.655	0.172
27273-1	0.278	0.317	0.129
27273-4	0.304	0.924	0.234
27273-5	0.252	0.97	0.3
27273-8	0.332	1.012	0.178
27273-10	0.279	0.509	0.117
AVERAGE	0.299	0.634	0.181
σ	0.158	0.248	0.069

6.4 STABLE ISOTOPE RESULTS

6.4.1 Introduction

Twenty-seven samples containing one or more of quartz, K-feldspar, carbonate (dolomite or calcite) and biotite were selected from six drill holes encompassing the length and a significant width of the drilled extent of the deposit (Figure 6.7). These phases were chosen because they are relatively abundant, because they span the alteration paragenesis, and therefore potentially chart changes in fluid provenance (if any), and because their fluid-mineral isotopic behaviour is relatively well constrained. The selected phases come mainly from veins, though in some instances replacement style only could be obtained (Table 6.12). Full sampling and analytical details are presented in Appendix C.

6.4.2 Fractionation equations used in this study

Isotope ratios are reported in the standard δ notation:

$$\delta = \frac{R_{sample} - R_{standard}}{R_{standard}} \times 1000 \text{ permil}$$

where R_{sample} is the relevant isotopic ratio being considered ($^{18}O/^{16}O$, D/H or $^{13}C/^{12}C$ in this study), and $R_{standard}$ is the corresponding ratio for the standard (SMOW or PDB).

The fractionation of isotopes between minerals and fluids with which they are in equilibrium is temperature dependent, and a number of such systems have been calibrated experimentally (see Table 25.1, p.462 in Faure, 1986 for a summary). Knowing the δ-value of a mineral, and having a reasonable, independent estimate of the temperature of mineral-fluid equilibration, one can calculate the δ-value of a fluid which coexisted with that mineral, or from which the mineral precipitated.

FIGURE 6.7: Sketch map of the Mount Dore prospect, showing locations of drill holes and isotope samples, projected to the surface. Sample identification is given as JCU number (minus 27- prefix), depth down drill hole (in metres), and phase(s) collected (**B** - biotite; **C** - carbonate; **K** - K-feldspar; **Q** - quartz).

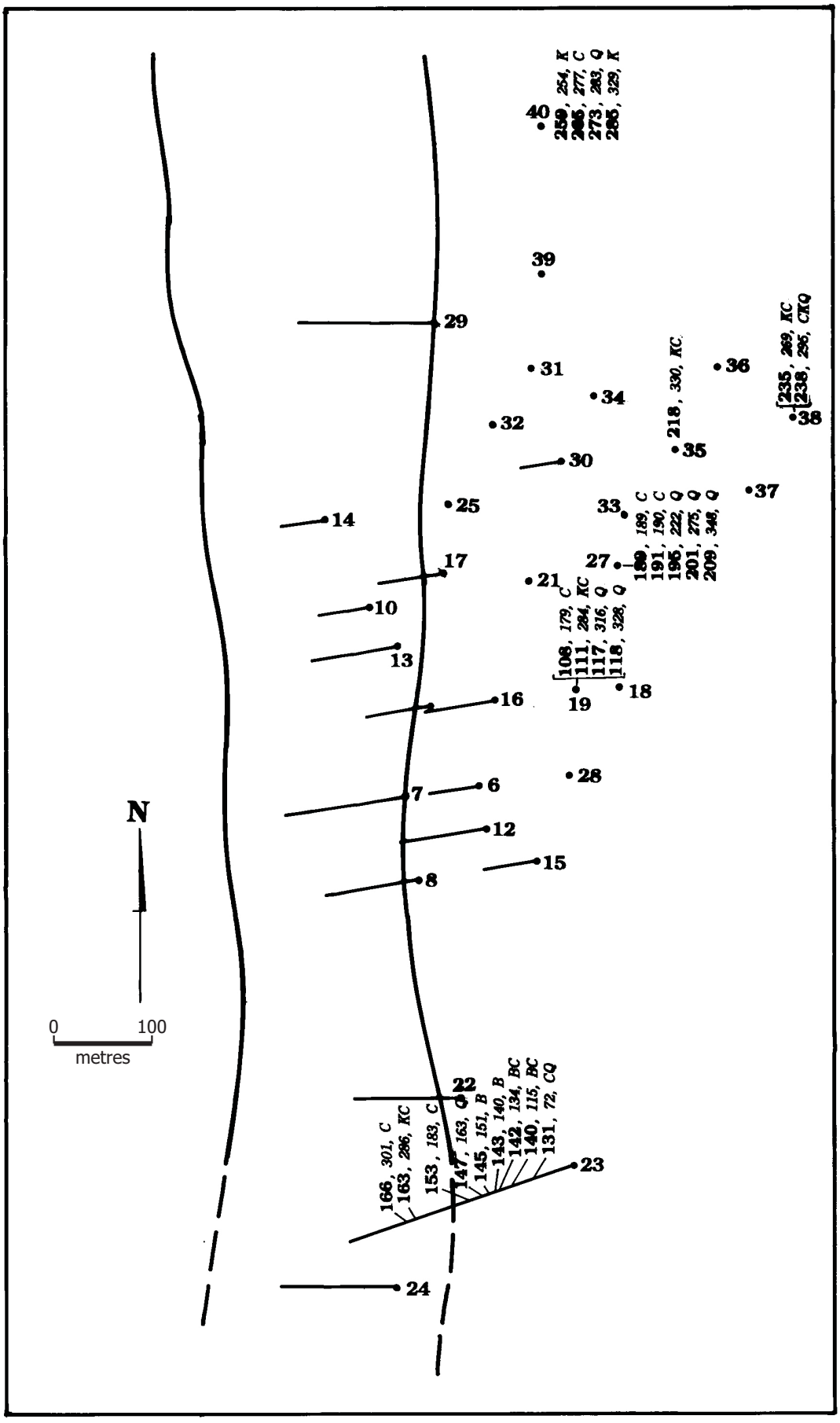

Mineral-water or mineral-CO_2 fractionation calculations in this study were performed using a simple programme written in Microsoft QuickBASIC (Appendix G), for use on a DOS-based personal computer. This programme gives the user the option of using one of several different calibrations for particular isotopic systems. The fractionation equations used are listed in Table 6.11.

The presence of highly saline primary fluid inclusions in quartz samples signifies that at least some quartz precipitated from highly saline fluids. Truesdell (1974) reported that increasing fluid salinity affects the mineral-water fractionation factor, but more recent experiments by Kendall *et al.* (1983) and Ligang *et al.* (1989) indicate that the oxygen isotope effects of salts may not be important at temperatures higher than 250°C, at least for fluids containing K, Na, Cl and F and having salinities up to 40 wt%. The calibration determined by Ligang *et al.* (1989) is employed for temperatures up to 550°C (the experimental limits), and that by Matsuhisa *et al.* (1979) for temperatures higher than this.

Attempts to calculate temperatures from mineral pairs gave inconsistent results, suggesting earlier formed minerals did not (fully) re-equilibrate with the later fluid. Equilibration temperature estimates are therefore made using fluid inclusion thermometry. These temperatures are poorly constrained, and a range of $\pm 100^{o}$ has been used to bracket the probable temperature of isotope equilibration for each of the minerals. The shifts in calculated fluid isotope composition arising from these temperature variations, for -100°C and +100°C are, respectively: **quartz $\delta^{10}O$:** -1.8 and +1.3 permil; **K-feldspar $\delta^{18}O$:** -0.9 and +0.5 permil; **biotite δD:** +7 and -10 permil; **dolomite $\delta^{18}O$:** -3.5 and +2.1 permil; **dolomite $\delta^{13}C$:** -1.3 and +0.5 permil; **calcite $\delta^{10}O$:** -3 and +1.9 permil; **calcite $\delta^{13}C$:** -1.1 and +0.4 permil. Results are presented in Table 6.12. The data sets are small, and averages are quoted below as medians and total errors, calculated using the sign test according to the recommendations of Rock *et al.* (1987).

TABLE 6.11: Mineral-fluid isotope fractionation calibrations used in this study. Equations are of the form:

$$1000\ln\alpha_{\text{mineral-fluid}} = A.10^{8}.T^{-3} + B.10^{6}.T^{-2} + C.10^{3}.T^{-1} + D \simeq \delta_{\text{mineral}} - \delta_{\text{fluid}}$$

where T is the absolute temperature (Kelvin); A, B, C and D are experimentally determined constants, and X_{Al}, X_{Mg} and X_{Fe} are the mole fractions of Al^{3+}, Mg^{2+} and Fe^{2+}, respectively, in the octahedral site in biotite.

MINERAL-FLUID PAIR	A	B	C	D	TEMPERATURE RANGE (^{o}C)	REFERENCES
$\delta^{18}O$						
quartz-H_2O	-	3.306	-	-2.71	180-550	Ligang *et al.* (1989)
	-	2.05	-	-1.14	500-800	Matsuhisa *et al* . (1979)
K-feldspar-H_2O	-	2.39	-	-2.51	400-500	Matsuhisa *et al.* (1979)
	-	1.59	-	-1.16	500-800	
calcite-H_2O	-	2.78	-	-2.89	0-500	O'Neil *et al* . (1969)
dolomite-H_2O	-	3.23	-	-3.29	100-600	Sheppard and Schwarcz (1970)
$\delta^{13}C$						
calcite-CO_2	-8.914	8.557	-18.11	8.27	0-600	Ohmoto and Rye (1979)
dolomite-CO_2	-8.914	8.737	-18.11	8.44	0-600	Ohmoto and Rye (1979) Sheppard and Schwarcz (1970)
δD						
[1]biotite-H_2O	-	-22.4	-	28.2 + ($2X_{Al}$-$4X_{Mg}$-$68X_{Fe}$	400-850	Suzuoki and Epstein (1976)
[2]biotite-H_2O	-	-21.3	-	-2.8	400-850	

[1] biotite composition known

[2] "average" biotite, of unknown composition.

TABLE 6.12(a): $\delta^{18}O_{SMOW}$ isotope results for K-feldspar and coexisting fluid. The calibration of Matsuhisa *et al.* (1979) was used. NA - sample supplied but not analysed.

SAMPLE NUMBER	LITHOLOGY	MINERAL "STYLE"	$\delta^{18}O$ ‰ (K-spar) (SMOW)	$\delta^{18}O$ ‰ (water) (SMOW)		
				450°C	550°C	650°C
27111	Brecciated and altered quartz-muscovite schist/phyllite	vein	NA	-	-	-
27163	Altered siliceous metasiltstone	replacement	11.9	9.8	10.7	11.2
27218	Silicified, brecciated slate or micaceous phyllite	vein±replacement	11	8.9	9.8	10.3
27235	Altered granite breccia	granitic	11.5	9.4	10.3	10.8
27238	Altered granite breccia	granitic	10	7.9	8.8	9.3
27259	Fractured carbonaceous slate	vein	12.3	10.2	11.1	11.6
27285	Silicified, laminated slate	vein	11.9	9.8	10.7	11.2

TABLE 6.12(b): δD_{SMOW} isotope results for biotite.

SAMPLE NUMBER	LITHOLOGY	MINERAL "STYLE"	δD (biotite) (SMOW)	δD (water) (SMOW)		
				450°C	550°C	650°C
27140	Biotite-calcite-quartz rock	replacement	-53	-21	-31	-38
27142	Biotite-calcite-quartz rock	replacement	-58	-14	-24	-30
27143	Biotite-calcite-quartz rock	replacement	-65	-21	-31	-37
27145	Altered metasiltstone	replacement	-53	-19	-29	-35

TABLE 6.12(c): $\delta^{18}O_{SMOW}$ isotope results for quartz and coexisting water. The calibration of Ligang *et al.* (1989) was used for 400 and 500°C, and that of Matsuhisa *et al.* (1979) for 600°C. NA - sample provided but not analysed.

SAMPLE NUMBER	LITHOLOGY	MINERAL "STYLE"	$\delta^{18}O$ ‰ (quartz) (SMOW)	$\delta^{18}O$ ‰ (water) (SMOW)		
				450°C	550°C	650°C
27116	Strongly silicified quartz-muscovite phyllite	vein±replacement	14.3	9.7	11.5	12.8
27117	Strongly silicified quartz-muscovite phyllite	vein	13.5	8.9	10.7	12.1
27118	Strongly silicified quartz-muscovite phyllite	vein±replacement	13.4	8.8	10.6	11.9
27131	Altered banded calc-silicate rock	vein±replacement	14.5	9.9	11.7	13
27147	Altered quartzo-feldspathic metasiltstone	vein±replacement	NA	-	-	-
27163	Altered siliceous metasiltstone	vein	15.1	10.5	12.3	13.6
27195	Altered and brecciated quartz-muscovite schist	vein	14.9	10.3	12.1	13.4
27199	Siliceous carbonaceous slate and micaceous phyllite	vein	14	9.4	11.2	12.5
27204	Altered and mineralized, brecciated carbonaceous slate	vein±replacement	NA	-	-	-
27209	Altered and brecciated carbonaceous slate	vein±replacement	13.8	9.2	11	12.3
27218	Silicified, brecciated slate or micaceous phyllite	vein±replacement	13.4	8.8	10.6	11.9
27235	Altered granite breccia	granitic	11.5	6.9	8.7	10
27238	Altered granite breccia	granitic	10	5.4	7.2	8.5
27273	Massive brecciated and mineralized quartz vein in carbonaceous slate breccia	vein±replacement	12.7	8.1	9.9	11.2

TABLE 6.12(d): $\delta^{13}C_{PDB}$ and $\delta^{18}O_{PDB\ and\ SMOW}$ analyses for carbonates.

SAMPLE NUMBER	LITHOLOGY	MINERAL SPECIES	MINERAL "STYLE"	$\delta^{13}C$ ‰ (mineral) (PDB)	$\delta^{18}O$ ‰ (mineral) (PDB)	$\delta^{18}O$ ‰ (mineral) (SMOW)	$\delta^{13}C$ ‰ (CO_2) (PDB)			$\delta^{18}O$ ‰ (water) (SMOW)		
							250° C	*350° C*	*450° C*	*250° C*	*350° C*	*450° C*
27108	Silicified quartz-muscovite phyllite breccia	ferroan dolomite	vein± replacement	-5.4	-8.2	19.4	-4.9	-3.6	-3.1	10.9	14.4	16.5
27111	Brecciated, altered quartz-muscovite schist/phyllite	ferroan dolomite	vein	-8.1	-3.2	24.5	-7.6	-6.3	-5.8	16	19.5	21.6
27131	Altered banded calc-silicate rock	calcite	vein± replacement	-5.4	-17.9	12.4	-4.1	-3	-2.6	5.1	8.1	10
27140	Biotite-calcite-quartz rock	calcite	replacement	-5.7	-17.5	12.8	-5	-3.3	-2.9	5.5	8.5	10.4
27142	Biotite-calcite-quartz rock	calcite	vein	-6.3	-20.1	10.1	-6.4	-3.9	-3.5	2.8	5.8	7.7
27153	Silicified quartz-muscovite phyllite	ferroan dolomite	vein± replacement	-6.9	-9.5	18	-6.3	-5.1	-4.6	9.5	13	15.1
27166	Altered, mineralized, milled breccia (siltstone precursor?)	ferroan dolomite	vein	-5.8	-10.7	16.8	-5	-4	-3.5	8.3	11.8	13.9
27189	Altered, mineralized quartz-muscovite schist breccia	dolomite	vein/infill	-5.3	-9.7	17.8	-5	-3.7	-3.2	9.3	12.8	14.9
27191	Altered, mineralized quartz-muscovite schist breccia	ferroan dolomite	vein	-6.4	-9.6	17.9	-5.9	-4.6	-4.1	9.4	12.9	15
27238	Altered granite breccia	ferroan dolomite	vein± replacement	-7.7	-11.6	15.9	-7.2	-5.9	-5.4	7.4	10.9	13
27265	Altered carbonaceous slate breccia	ferroan dolomite	vein	-6.1	-9.9	17.6	-5.6	-4.3	-3.8	9.1	12.6	14.7

6.4.3 Results

Oxygen

$\delta^{18}O_{SMOW}$ values were determined for four K-feldspar samples from veins or replacement in metasediments, and for two from undisrupted, yet altered Mount Dore Granite (Table 6.12a). The results define a single population having an average of $11.7^{+0.4}_{-1.7}$. This corresponds to a $\delta^{18}O_{SMOW}$ for the hydrothermal fluid of $10.5^{+0.4}_{-1.7}$. K-feldspar alteration formed earlier than quartz in the paragenesis, and the equilibrium temperature is therefore assumed to have been 550°C, slightly hotter than conditions at quartz precipitation (500°C; see below).

Twelve samples of quartz were analysed for $\delta^{18}O$ (Table 6.12c). Ten of these are of the vein and replacement style, and define an apparently uniform population having a median $\delta^{18}O$ of $13.9^{+1.0}_{-0.5}$ permil. Two samples of quartz from altered Mount Dore Granite, however, are lighter by 2 to 3 permil, and are treated as a separate population, with a median $\delta^{18}O$ of 10.75 $\pm$ 0.75 permil. Quartz precipitated after K-feldspar in the alteration paragenesis. A slightly cooler equilibrium temperature of 500°C is used, to obtain a fluid $\delta^{18}O$ of $11.1^{+1.0}_{-0.5}$ permil for the vein-replacement population, and a $\delta^{18}O$ of 7.95 $\pm$ 0.75 permil for granitic quartz.

Eight samples of dolomite yielded a tightly constrained population of $\delta^{18}O_{SMOW}$ values with a median of $17.85^{+1.55}_{-1.05}$ permil ($\delta^{18}O_{PDB}$ median $-9.65^{+1.55}_{-1.05}$ permil; Table 6.12d). This corresponds to a fluid $\delta^{18}O_{SMOW}$ of $12.85^{+1.55}_{-1.05}$ permil, for an equilibrium temperature of 350°C. There is no apparent difference in isotopic composition between ferroan and non-ferroan dolomite. The lowest $\delta^{10}O$ value for dolomite is from sample 27238, which contains some calcite (from XRD analysis; S. Golding pers. comm.). The highest value appears to be anomalous, but the median and errors quoted for all eight values is unchanged if the highest and lowest values are disregarded. The three samples of calcite had notably less ^{18}O than dolomite. The median $\delta^{18}O_{SMOW}$ was $12.4^{+0.4}_{-2.3}$ permil ($\delta^{18}O_{PDB}$ median $-17.9^{+0.4}_{-2.2}$ permil), which corresponds to a fluid $\delta^{18}O_{SMOW}$ of $8.1^{+0.4}_{-2.3}$ permil, for the same equilibrium temperature (Table 6.12d).

Deuterium

Biotite is the only hydroxyl-bearing alteration phase abundant enough to extract for deuterium analyses. It occurs as replacement only, in a similar position in the alteration paragenesis to K-feldspar. It is assumed to have equilibrated with the same fluid as the alkali feldspar, at the same temperature ($550 \pm 100^{o}C$).

Two biotite-water calibrations are available. One requires information on the mole proportions of Al^{3+}, Fe^{2+} and Mg^{2+} in the octahedral lattice sites. The other does not require compositional data, but is inherently less accurate. Two of the biotite samples were analysed by microprobe during mineral geochemistry studies (Table 5.11). Sample JCU-27140 most closely approaches unaltered biotite (tetrahedral, octahedral and interlayer sites occupied to roughly the expected degree). Sample JCU-27145 shows signs of alteration, probably to chlorite. There are no compositional data for the other two samples, but they are all from the same type of altered rock, and are probably similar in composition. The unanalysed biotites are lighter in colour (more chloritized?; S. Golding, Qld. Univ., pers. comm.), and also marginally lighter in deuterium, but the δD values for all samples are tightly constrained about a median value of $-56.5^{+3.5}_{-8.5}$ permil. The corresponding δD values for water are also tightly constrained, with a median value of $-25^{+6}_{-1.0}$ permil.

Carbon

Results of carbon isotope analyses of carbonates are recorded in Table 6.12d. The median $\delta^{13}C_{PDB}$ value for the eight dolomite analyses is $-6.25^{+0.85}_{-1.45}$ permil, which corresponds to a median fluid $\delta^{13}C_{PDB}$ of $-4.45^{+0.75}_{-1.45}$ permil at a temperature of $350^{o}C$. Again, there is no apparent difference in isotopic composition between ferroan and non-ferroan dolomite. The three calcite analyses yielded a marginally heavier median $\delta^{13}C_{PDB}$ of $-5.7^{+0.3}_{-0.6}$ permil, which corresponds to a fluid $\delta^{13}C_{PDB}$ of $-3.3^{+0.3}_{-0.6}$ permil, for the same equilibrium temperature.

Sulphur

No sulphur isotope analyses were made in this study, but Scott (1986) reported his results from disseminated and vein pyrite from the mineralized and footwall intervals at Mount Dore, and these are recorded herein for completeness. Pyrite associated with mineralization has $\delta^{34}S$ values of -2 to +5 permil (average 2.9 permil; four values), presumably measured relative to troilite in the Canyon Diablo meteorite, although this is not explicitly stated. Footwall pyrite is significantly heavier at 12 permil. The complete data are not presented, and the positions of his pyrite groups within the overall paragenesis are poorly constrained.

6.5 DISCUSSION

6.5.1 Primary fluid composition

Primary Type I multiphase solid inclusions cannot have trapped the "real" primary fluid, because the host quartz precipitated after an earlier episode of potassic metasomatism produced K-feldspar and biotite. Unfortunately, potassic phases have not trapped useful inclusions, and so primary inclusions in quartz remain the nearest to original fluid composition available for study. It is also likely that Type I multiphase solid inclusions have not trapped a truly representative sample of the fluid from which the quartz host precipitated. These inclusions are coeval with H_2O-CO_2 inclusions, and probably also with halite solid inclusions. This association suggests that at least two fluid phases of grossly different bulk composition were present and trapped simultaneously. There are two possible explanations for this relationship.

The first is that the two fluids were derived from separate sources, and were channelled into favourable dilatant zones at Mount Dore, where they subsequently mixed to form the range of inclusion types observed. There is no evidence, however, for CO_2 in any inclusions trapped later in the paragenesis, and mixing of two separate fluids is therefore deemed unlikely.

The more attractive possibility is that the two fluid inclusion populations contain fluids formed by unmixing from a single homogeneous fluid as physical conditions fell below the solvus for that fluid. Immiscibility in the H_2O-CO_2 system occurs only at temperatures less than about 350°C for pressures less than 200 MPa, far lower than the 500°C+ suggested by fluid inclusion thermometry, but addition of salt is known to raise the solvus temperature. Phase relations in the CO_2-H_2O-salt system are still poorly understood, however, although approximate P-T-X topologies for the CO_2-H_2O-NaCl system at various pressures and NaCl concentrations have been derived by Gehrig (1980) and Bowers and Helgeson (1983), and show that the solvus consolute temperature may be raised several hundred degrees Celsius by the presence of dissolved salts (Figure 6.8).

The extraordinarily high salinity Type I multiphase solid inclusions therefore probably represent the salt-rich aqueous phase which unmixed from a single lower-salinity, CO_2-bearing phase. Phase separation may have resulted from cooling of the fluid, or alternatively have been initiated by an abrupt decrease in pressure associated with fault rupture. The formation of halite solid inclusions could have precipitated as partitioning of salts into the aqueous phase caused oversaturation of NaCl in the solution. The immiscible saline aqueous and H_2O-CO_2 fluids will have significant differences in physical properties (density, viscosity, surface tension, *etc.*), and it is therefore possible for them to become physically segregated, and for the CO_2-rich phase to be preferentially lost from the system (Trommsdorff and Skippen, 1986).

The "primary" fluid present just prior to quartz precipitation therefore would have been a still very saline (up to 60 weight percent salt?) solution containing significant amounts of CO_2. The mole proportion of CO_2 in the original primary fluid is impossible to assess from the available data. Most observed examples of CO_2-bearing inclusions were apparently trapped after phase separation. One example of an inclusion containing multiple daughters, an aqueous solution **and** liquid and gaseous CO_2 was observed (Figure 6.1g), but no useful geochemical information could be obtained.

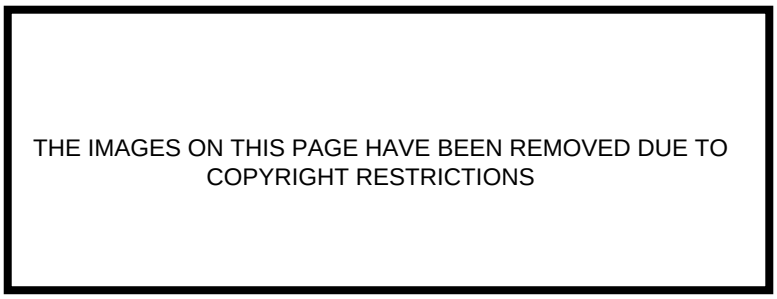

FIGURE 6.8: T-X_{CO2} diagrams for 35 weight percent NaCl relative to H_2O + NaCl, for a variety of confining pressures. Note that the addition of significant proportions of salt to an H_2O-CO_2 fluid raises the solvus consolute temperature several hundred degrees above that of the salt-free system (*ca.* 350°C at 200MPa), consistent with observations of immiscibility in fluid inclusions from Mount Dore at elevated temperatures (>500°C). Diagram is after Figure 13 of Bowers and Helgeson (1983).

The prevalence of CO_2 over CH_4 as the carbon-bearing species, and the precipitation of haematite with microcline indicates the early, high-temperature fluid was relatively oxidized. Any sulphur present would therefore also have been predominantly as an oxidized species, an important consideration when considering metal transport and precipitation mechanisms (see Section 6.5.3).

6.5.2 Evolution of fluid chemistry from fluid inclusion evidence

The earliest recognized fluid clearly associated with alteration in the Mount Dore system was a high temperature (>500^{o}C), extremely saline (up to 70 weight percent salt) solution containing a variety of solute species (Na^{+}, K^{+}, Fe^{2+}, Ca^{2+}, Cl^{-}, CO_3^{2-} and probably a host of less abundant ones), and also CO_2. The presence of CO_2, and haematite as rare trapped solids in the primary fluid inclusions, indicate that the fluid was relatively oxidizing (above the CH_4-CO_2 and haematite-magnetite buffers).

At the time of earliest quartz precipitation the single fluid phase separated into a highly saline aqueous phase, and a lower salinity CO_2-rich phase, which being more mobile was largely carried away from the system. Immiscibility may have resulted from a combination of temperature and pressure decrease accompanying adiabatic expansion of the fluid into ruptures created during movement along the Mount Dore Fault Zone. SiO_2 saturation may have been caused in part by removal of some H_2O in the CO_2-rich phase; *i.e.* phase immiscibility, quartz precipitation and inclusion trapping were related processes.

The remaining fluid progressively evolved towards lower temperatures and salinities. Dilution might be partly explained by boiling, and this is supported by abundant vapour-rich inclusions. Thermometric data are still sparse, however, and unequivocal evidence therefore lacking, although loss of residual CO_2 to a vapour phase is a possible mechanism for carbonate precipitation. In any case, boiling alone would result in salt saturation for all compositions. Fluid close to or exceeding salt saturation only appears to have been present in the very early stages of alteration, and

later fluids are distinctly undersaturated. These must have been physically diluted by addition of another, salt-undersaturated phase. Eutectic temperatures indicate that low salinity fluids still contained divalent solute species.

6.5.3 Transport and precipitation of base metals

Transport of base and precious metals (Cu, Zn, Pb, Ag) at elevated temperatures is conventionally regarded to be by chloride or sulphide complexes (Barnes, 1979). The primary fluid at Mount Dore was a highly saline, oxidized chloride brine, probably poor in reduced sulphur. Chloride complexes are therefore likely to have been dominant. No estimates of base metals concentrations in the fluid were obtained, but ore-producing fluids reported from elsewhere contain tens to thousands of ppm dissolved metals (Roedder, 1979; Barnes, 1979). Deposition of base metal (Me^{2+}) sulphides from chloride complexes may be represented by a reaction of the sort:

$$MeCl_2\,(aq) + H_2S\,(aq) \;===\; MeS + 2H^+ + 2Cl^-$$

(Barnes, 1979). Precipitation may be induced by (i) cooling the fluid, (ii) reducing the activities of complexing ligands, (iii) increasing the activity of S^{2-}, or (iv) increasing the fluid pH (Crerar and Barnes, 1976; Barnes, 1979). Fluid inclusion evidence indicates that the fluid was cooling and becoming more dilute with time. Fluid pH may be increased by boiling off acid gases, or by consumption of H^+ by reaction with carbonate. Evidence for boiling is equivocal, but replacement of carbonate certainly occurs many parts of the prospect. Mechanisms (i), (ii) and (iv) may therefore all have played a part in sulphide deposition. The controlling factor, however, appears to have been the availability of reduced sulphur. Replacement, or at least close spatial association of pyrite with base metal sulphides strongly suggests the fluid was very poor in H_2S, which had to be scavenged instead from the earlier sulphide.

6.5.4 Fluid provenance

Fractionation considerations

Calculations of fluid stable isotope ratios from those of alteration minerals for provenance studies assume that these minerals precipitated from and were at that time in isotopic equilibrium with a homogeneous fluid, and that the element whose isotopic ratio is to be determined was contained in only one component of the fluid. Complications arise if a particular element is partitioned between several components, because mineral-fluid fractionations are calculated for only one of these, and the ratio thus derived is not representative of the bulk fluid.

Fluid inclusion evidence from Mount Dore indicates that the primary hydrothermal fluid belonged at least to the H_2O-CO_2-salt system. Phase behaviour during thermometric studies did not reveal significant amounts of other carbon or hydrogen-bearing components (CH_4, H_2S). It probably existed as a single homogeneous phase during early K-feldspar (and biotite?) alteration, but during later quartz precipitation had separated into two immiscible phases - a saline aqueous liquid and a CO_2+H_2O vapour. The effects of isotope partitioning between different components or phases for each of these stages are broadly similar in principle, but differ slightly in detail.

For the homogeneous fluid stage, hydrogen and carbon isotope ratios may be calculated using known mineral-H_2O and mineral-CO_2 fractionation factors, since each element would have been wholly contained in either the H_2O or CO_2 component. No carbonate minerals were precipitated at this stage. The hydrogen isotope ratio calculated from that of biotite will therefore reflect the hydrogen provenance for the fluid, provided the biotite has not re-equilibrated with subsequent fluids (see below). Oxygen isotopes, however, will be partitioned between the H_2O and CO_2 components. CO_2 preferentially concentrates ^{18}O relative to H_2O (Truesdell, 1974), and the $\delta^{18}O$ for H_2O will therefore always be lower than that of the bulk fluid. Fluid $\delta^{18}O$ ratios calculated using mineral-H_2O fractionation factors are therefore those of the H_2O

component of the fluid, and this will only be close to the bulk value for low mole fractions of CO_2 (Bowers, 1991).

The situation is more complicated when immiscibility occurs, because each phase is not a pure component, but a mixture of several components dominant in a particular species. Hydrogen and carbon may also fractionate between liquid and vapour phases. If quartz equilibrated only with the aqueous phase, the calculated fluid ^{18}O signature will be for this fluid, and will be lower than that for the primary (bulk) fluid.

The magnitude of the difference in $\delta^{18}O$ will depend on the mole fraction of CO_2 relative to H_2O and the temperature. To calculate ^{18}O for the bulk fluid, one needs to know these parameters, and also the fractionation factors for mineral-H_2O and mineral-CO_2 systems (Bowers, 1991). Mineral-H_2O oxygen isotope fractionation factors are reasonably well constrained for many common silicate and carbonate minerals (see, for example, the compilation in Table 25.1 of Faure, 1986), but ^{18}O fractionation in mineral-CO_2 systems are unknown.

For H_2O-CO_2 systems having initial CO_2 mole fractions less than 0.15, and at temperatures less than 300°C and pressures less than 150 MPa, subsolvus $\delta^{18}O$ depletions of less than 4 permil arise in the aqueous phase relative to the bulk value (Bowers, 1991). Depletion of $\delta^{18}O$ in the H_2O component in a single homogeneous phase is likely to be of similar magnitude. Higher temperatures will reduce the fractionation factor, and hence the depletion (for similar CO_2 mole fractions). The effects of increased salinity on isotope fractionation in H_2O-CO_2-salt-mineral systems are unknown. Ligang *et al.* (1989) detected no salinity effects on isotope ratios in the quartz-H_2O-salt system for salt concentrations up to 40 weight percent and temperatures up to 550°C. In the absence of experimental data on CO_2-bearing systems, salinity effects are assumed to be negligible.

Existing data therefore suggest that for the H_2O-CO_2-salt system, the $\delta^{18}O$ for the H_2O component of a single homogeneous phase, or for the saline aqueous fluid

coexisting with an immiscible CO_2-rich phase at elevated temperatures will have a $\delta^{18}O$ at most only a few permil lower than the bulk system, unless the latter contained a significant initial mole fraction of CO_2 (X_{CO_2}>0.15).

The temperature of the primary fluid at Mount Dore is constrained by fluid inclusion microthermometry to 500$\pm$100^{o}C, but there are insufficient data to determine the original mole fraction of CO_2. The rarity of CO_2-bearing inclusions in the Mount Dore system suggests low initial CO_2 mole fractions, but CO_2-rich fluids are likely to be extremely mobile in an active faulting regime, and the original CO_2 content may have been high. The fluid was also demonstrably relatively oxidizing, and CO_2 may have been replenished by reaction of water with graphite released to the fluid during alteration. This would further reduce the $\delta^{18}O$ of the remaining H_2O, by 1 to 2 permil (Lynch *et al.*, 1990). Further work is clearly desirable.

Even without knowledge of CO_2 mole fractions, however, one conclusion which can be reached is that the bulk primary fluid could only have been isotopically heavier than recorded from mineral isotopic ratios, perhaps by several permil (or more?).

Fractionation of $\delta^{34}S$ between different sulphur species in the hydrothermal fluid must also be considered. The proportions of oxidized and reduced species will vary with f_{O_2} in the fluid. If this lies at or above the haematite-magnetite buffer, oxidized sulphur (mainly SO_2 or SO_4^{2-}, depending on temperature) will be dominant over reduced sulphur (largely H_2S), and the $\delta^{34}S_{H_2S}$ value derived from sulphide mineral isotopic analyses can be as much as 10 permil (where SO_2 is dominant) to 30 permil (where SO_4^{2-} prevails) lower than that of $\delta^{34}S_{fluid}$ (Ohmoto and Rye, 1979).

Source of oxygen

The $\delta^{18}O_{SMOW}$ values derived from microcline and quartz for the primary fluid are very similar at 10.5 to 11.1$^{o}/_{oo}$, except for those derived from "granitic" quartz,

which are significantly lower (by 2 to 3‰). The primary hydrothermal fluid was therefore much heavier than common meteoric waters and SMOW, but all values lie within or very close to both the magmatic and metamorphic field of Taylor (1974; see Figure 6.9). Distinction between the two possibilities requires knowledge of the fluid δD (see below). The lower fluid $\delta^{18}O$ value derived from "granitic" quartz possibly indicates that this is an original magmatic phase which did not fully re-equilibrate with the hydrothermal fluid. Its ^{18}O content may reflect the original magmatic value, and if so, the hydrothermal fluid cannot have been derived either from or by interaction with the Mount Dore Granite, because it would have a lower $\delta^{18}O_{SMOW}$ than the quartz.

Carbonate alteration equilibrated with a later, salt-undersaturated, CO_2-poor, aqueous fluid believed to be the descendent of the salt-saturated aqueous immiscible phase from which quartz precipitated. It should therefore have the same $\delta^{18}O$, yet the calculated $\delta^{18}O$ in equilibrium with the dolomite is significantly heavier (by more than 2‰) than that for early fluid. This difference may be evidence of either boiling, fluid mixing or fluid-rock interaction. Boiling produces a residual liquid isotopically heavier than the bulk fluid because water vapour concentrates the lighter isotopes of oxygen and hydrogen. Extensive boiling, however, will maintain salt saturation in the liquid phase. Mixing with another isotopically heavier, dilute liquid could produce the same isotopic effect, and also produce the observed dilution trend. Exchange of oxygen with host rock during early alteration may also have contributed. The isotopic signature is still clearly that of a metamorphic or magmatic fluid (Figure 6.9).

Calcite apparently formed from a fluid some 4‰ lighter in ^{18}O than dolomite, and more than 2‰ lighter than that producing microcline. The reason for this is not clear. Calcite and dolomite are interpreted to have formed contemporaneously, and the difference may reflect differences in the physical conditions of formation from north to south, or could indicate exchange with Staveley Formation rocks, which would presumably have had a lower $\delta^{18}O$ than the fluid.

FIGURE 6.9: Deuterium and oxygen isotope results for samples from Mount Dore. The field in pale shading indicates the total range of ä^{18}O obtained from the specimens, including standard deviations, for the temperatures selected (350-550°C) for each set of mineral-fluid isotope calculations. The dark shaded region denotes the D-O isotopic character interpreted for the "primary" hydrothermal fluid, defined by the äD and ä^{18}O values derived from biotite and K-feldspar, respectively, assuming that these phases formed at the same time, and that biotite äD has not been affected by subsequent fluids. Fields of primary magmatic and metamorphic H_2O are those recommended by Taylor (1974), and the primary hydrothermal fluid at Mount Dore clearly appears to have had a deep-seated metamorphic origin (see Section 6.5.4 for discussion).

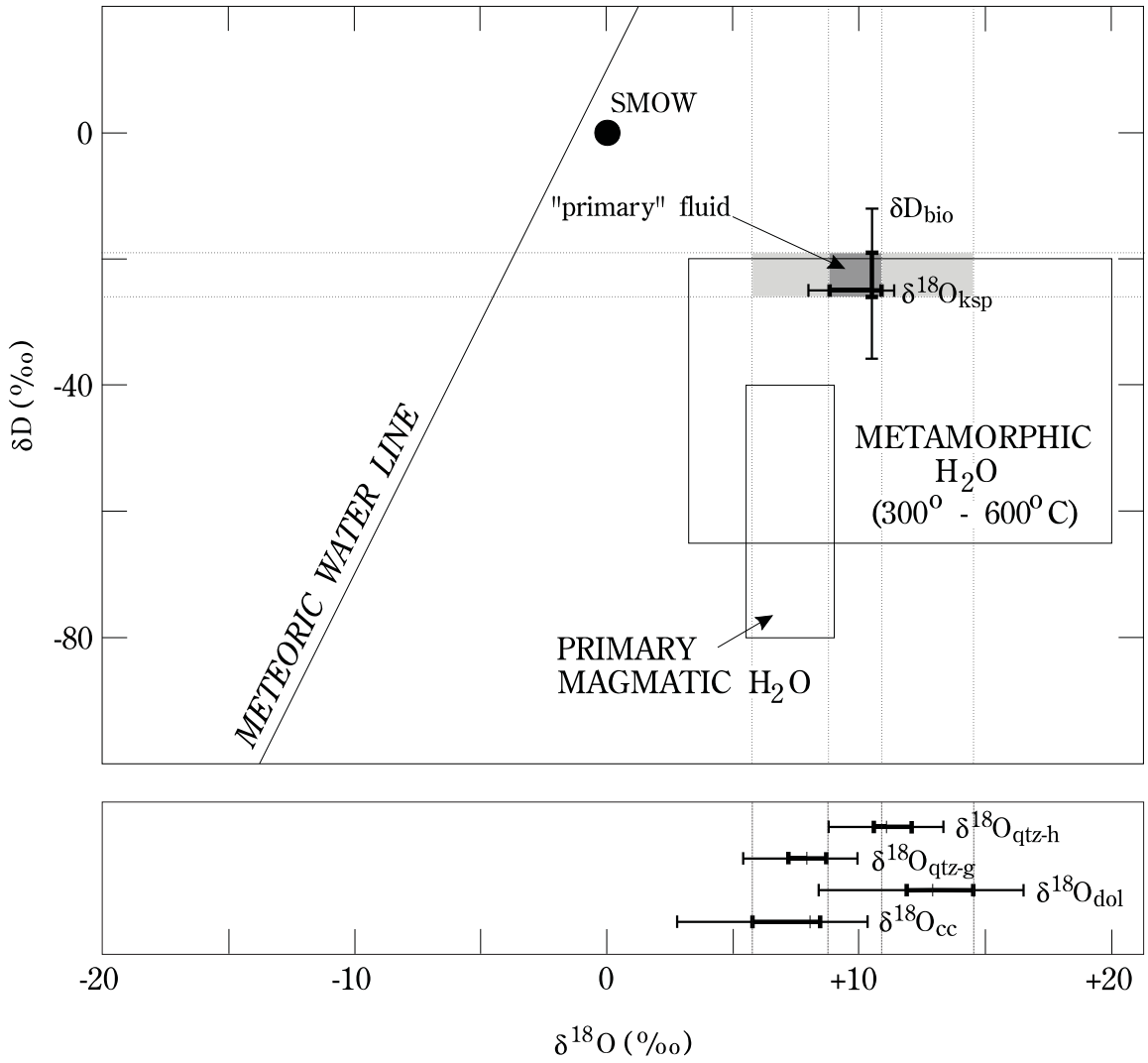

Source of deuterium

Hydrogen isotopic data remain sparse, but the dominant hydrogen-bearing alteration phase biotite is relatively uncommon, and so its δD signatures will therefore most clearly indicate that of the hydrothermal fluid. Biotite appears to have formed at the same time as the microcline, though this timing is not satisfactorily constrained. The fluid δD derived from biotite is clearly heavier than expected for a magmatic fluid. If this δD, and $\delta^{18}O$ data derived from microcline or quartz are assumed to relate to a single fluid, this fluid plots well to the right of the meteoric water line, in the upper part of the metamorphic field (Figure 6.9).

The fluid is assumed to have been a single homogeneous phase at the time of biotite formation (before quartz), so fractionation of deuterium between immiscible phases need not be considered. Even if biotite should have formed at the same time or after quartz, however, fractionation of hydrogen isotopes through immiscibility yields an H_2O-dominant phase at most only a few permil heavier than the bulk fluid (Bowers, 1991). A bulk fluid δD value several permil lighter than measured will not alter the interpreted metamorphic provenance.

Unfortunately, hydrous minerals in ore deposits may have their H isotopic ratios changed by interaction with late-stage fluid (Ohmoto, 1986), and at Mount Dore there was ample opportunity for re-equilibration of biotite with such fluids. Even if this occurred, however, the late fluid must still have had a metamorphic isotopic signature. This is consistent with the interpreted fluid provenance from $\delta^{18}O$ and $\delta^{13}C$ analyses of the carbonates.

Source of carbon

Hoefs (1980) and Faure (1986) cite the primary sources of carbon in hydrothermal fluids as marine carbonates ($\delta^{13}C_{PDB}$ _ $0^{o}/_{oo}$), deep-seated or average crustal sources ($\delta^{13}C_{PDB}$ _ $-7^{o}/_{oo}$) and biogenic organic compounds ($\delta^{13}C_{PDB}$ _ $-25^{o}/_{oo}$).

The isotopic composition of CO_2 in solution also depends, however, on oxygen fugacity, pH, temperature, ionic strength of fluid and total concentration of carbon (Ohmoto, 1972; Rye and Ohmoto, 1974). These factors may vary in such a way as to produce CO_2 with a $\delta^{13}C$ significantly different from that of the bulk fluid.

The variation in $\delta^{13}C$ of CO_2 in solution relative to that of the bulk fluid is shown in Figure 6.10 as a function of f_{O_2} and pH, for the case where the temperature is 350°C (estimated from fluid inclusions) and the $\delta^{13}C$ of the total carbon in solution is 0‰. The stability fields of calcite and graphite are also shown, for a total carbon content in the fluid of 3.0 mol.kg^{-1} H_2O. This value may be somewhat high; lower concentrations cause the graphite field to shrink, and the calcite boundary to shift to the right.

The f_{O_2} and pH of the fluid from which carbonates precipitated can be approximated from phase parageneses and fluid inclusion data (Figure 6.10). Primary fluid inclusions preserve a CO_2-bearing fluid with little or no CH_4. CO_2 continued to predominate in the later fluid, because graphite which dissolved during early alteration remained in solution, and iron-oxides remained stable when carbonates later precipitated. Oxygen fugacities greater than about 10^{-30} atmospheres are indicated (for 350°C), and must have initially been considerably higher than this, because interaction with graphitic rocks of the Toole Creek Volcanics did not push the fluid redox state into the graphite-stable field. For such conditions the $\delta^{13}C$ values of carbonates and fluid vary largely as a function of pH only (Figure 6.10). Muscovite is occasionally observed associated with carbonate, and may be used to constrain the fluid pH. The muscovite stability field is also illustrated in Figure 6.10, for K^+ concentrations between m_{K^+} = 1.0 and 0.001 mol.kg^{-1} H_2O (suggested by Ohmoto (1972) as the likely range of concentrations for most mineralizing solutions).

A region in f_{O_2}-pH space is defined where the $\delta^{13}C$ of CO_2 varies by no more than 0.5‰ from that of the bulk fluid. Decreasing the temperature does not alter this result (Ohmoto, 1972). The fluid $\delta^{13}C$ therefore was in fact slightly depleted in ^{13}C relative to PDB, suggesting a deep-seated or average crustal origin for the carbon.

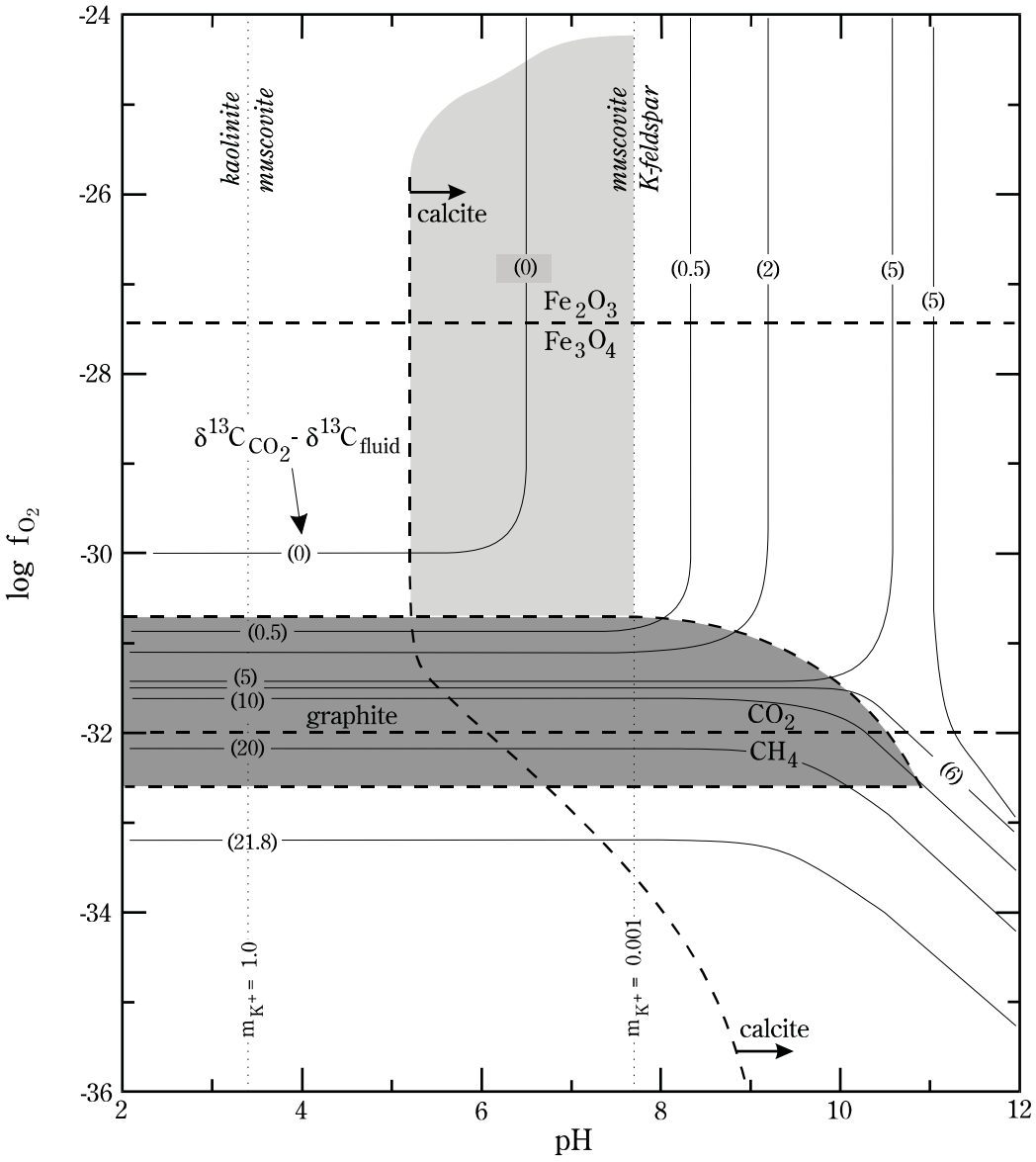

FIGURE 6.10: Deviation of $\delta^{13}C$ of CO_2 in solution from that of the bulk fluid, as a function of f_{O_2} and pH, for a temperature of 350°C (*i.e.* about that determined from fluid inclusion studies), and a $\delta^{13}C$ for the total carbon in solution of $0^{o}/_{oo}$. The stability fields of calcite and graphite are also shown, for a total carbon concentration in the fluid of 3.0 mol.kg^{-1} H_2O. The muscovite stability field is also illustrated, for K^+ concentrations between 1.0 and 0,001 mol.kg^{-1} H_2O. Mineralogical evidence from the Mount Dore system suggests that the $\delta^{13}C$ of CO_2 as calculated from mineral-fluid equilibria would have varied by no more than $\pm 0.5^{o}/_{oo}$ from that of the bulk fluid, supporting the interpretation of a deep-seated metamorphic derivation. Diagram is modified after Figure 13 of Ohmoto (1972).

Discrimination between igneous, sedimentary, or even mantle sources is equivocal, as partial melts of all these rocks would have $\delta^{13}C_{PDB}$ values around -5 to -10‰, and a coexisting magmatic or metamorphic fluid would have a similar value (Deines and Gold, 1973; Ohmoto and Rye, 1979).

The fluid $\delta^{13}C_{PDB}$ value calculated from calcite is marginally higher than that for fluid from which dolomite precipitated. The reason for this is also unclear, but calcite is most common in Staveley Formation rocks in the southern part of the prospect, and the difference may indicate contributions from primary carbonate from the Staveley Formation, which would be isotopically heavier than the fluid. Alternatively, calcite may have precipitated later, from a fluid enriched in ^{13}C by earlier dolomite formation.

Source of sulphur

The $\delta^{34}S$ data determined by Scott *et al.* (1984) for hydrothermal pyrite indicate a $\delta^{34}S_{H2S}$ value for the fluid of close to 0‰, leading Scott (1986) to conclude that the sulphur came from magmatic sulphides in the granite. This $\delta^{34}S_{H2S}$ will only be close to the value for the bulk fluid, however, if H_2S is the dominant species. The major factors which control sulphur isotope compositions in hydrothermal fluids are temperature, source of sulphur, and proportions of oxidized and reduced sulphur species (Ohmoto, 1972).

The early precipitation of haematite, and the lack of pyrite indicates the f_{O_2} of the fluid lay above the haematite-magnetite buffer, and that sulphur was largely SO_2 (Figure 6.11). Pyrite was precipitated only when reduced sulphur became available, perhaps (probably?) through reduction of oxidized sulphur by carbon released from slates during alteration. The true $\delta^{34}S_{fluid}$ will depend on the proportion of reduced sulphur produced at this time. If all was converted to H_2S a magmatic source is probable, but if only a small fraction was converted, the bulk fluid could have been significantly heavier ($\delta^{34}S_{fluid} > 10$‰?), and a (metamorphosed) sedimentary sulphide

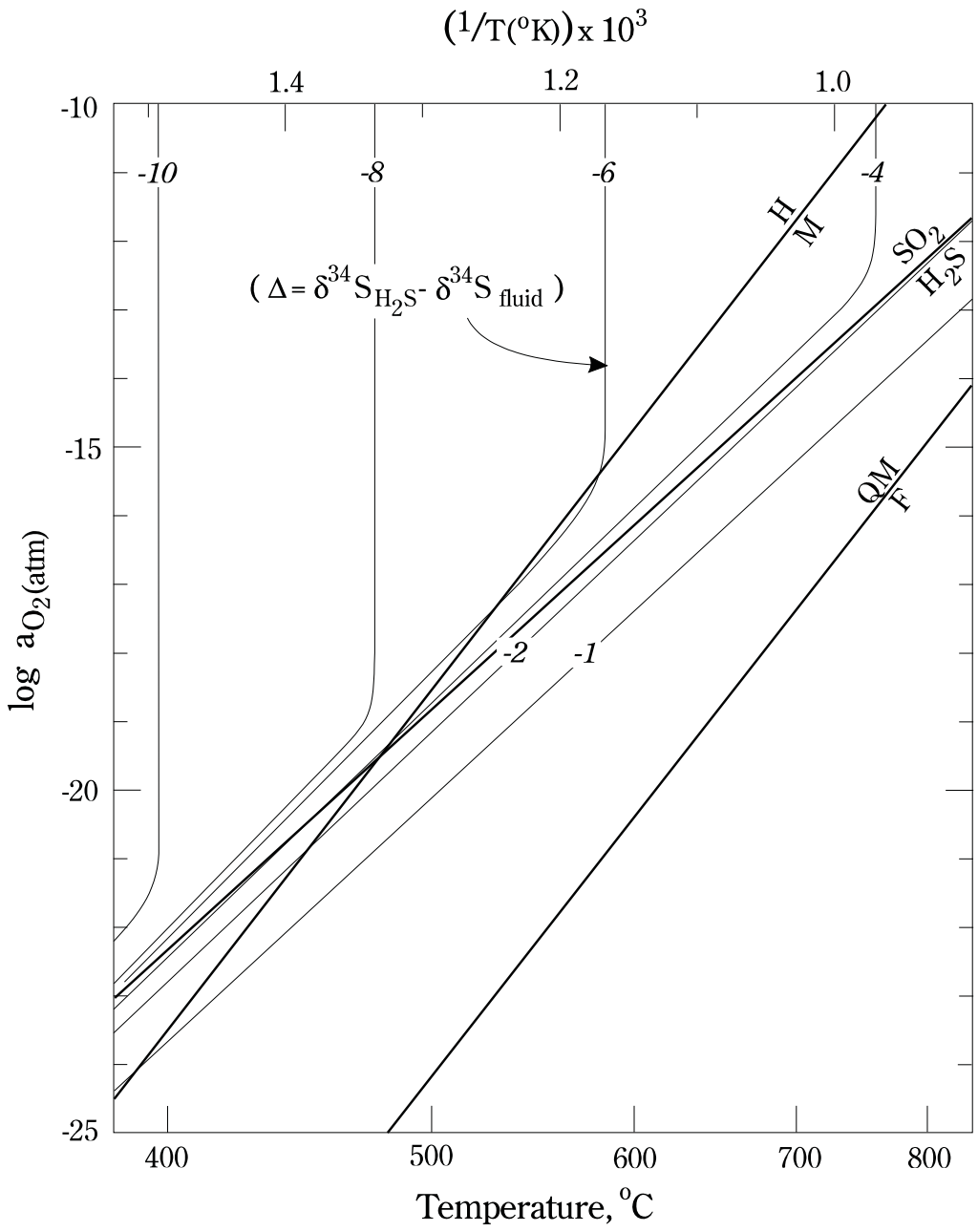

FIGURE 6.11: Deviation of $\delta^{34}S_{H2S}$ from $\delta^{34}S_{fluid}$ in high temperature hydrothermal fluids of P_{H_2O} = 100 MPa, as a function of log a_{O_2} and temperature. Note that $\delta^{34}S$ values determined from sulphide-H_2S equilibria may be lower than the bulk fluid value by up to $10^{o}/_{oo}$ (or more!) if other sulphur species (such as SO_2 or SO_4^{2-}) are present in significant amounts. This has possibly been the case at Mount Dore. Diagram modified after Figure 10.7 of Ohmoto and Rye (1979).

or sulphate source is possible. $\delta^{34}S$ values for footwall pyrite were considerably heavier at up to $12^{o}/_{oo}$, strongly suggesting a sedimentary source for the sulphur there. It is clear from the foregoing discussion that different sources of sulphur may not be necessary for pyrite in different parts of the Mount Dore Prospect. Further sulphur isotope studies are highly desirable.

Which means the fluid is...?

The earliest recognized ("primary") hydrothermal fluid was a hot, highly saline H_2O-CO_2 phase with an oxygen isotopic character indicating a reasonably clearly defined deep-crustal origin. Unequivocal discrimination between a metamorphic and magmatic sources (favouring the former) is only possible, however, if the biotite δD values have not been reset, which is probably unlikely.

Compositional data also allow equivocal sources. The primary fluid at Mount Dore is similar to those identified in other granite-associated settings (*e.g.* Brown *et al.*, 1984: granitic quartz - 69 wt% salt (average of 26 calculations); Eadington, 1983: Mole granite, New South Wales - 50-60 wt% salt; Kwak *et al.*, 1986, and references cited in Table 1 therein; Witt, 1988: Go Sam Granite, North Queensland - up to 70 wt% salt). The implied source for most of these fluids is magmatic. Compositionally similar fluids may, however, be derived by a number of other mechanisms. Highly saline (up to 50 wt%) metamorphic fluids may form by involvement in retrograde (rehydration) reactions with the rocks through which they are passing (Bennett and Barker, 1992), or by prograde reactions in salt- and carbonate-rich (*i.e.* evaporitic) sediments, or by moving into and leaching salts from such sediments.

The Mount Dore Granite was solid (though possibly still hot), and was itself extensively altered during the faulting and hydrothermal alteration event, suggesting that it was not the source of the fluid. Later granites may be responsible, but there is no evidence for these. An alternative is that magmatic fluid exsolved from the Mount Dore Granite deeper in the crust, and travelled as a separate phase, finally escaping

only when a pathway was provided by the faulting which controlled final, solid-state emplacement of the Mount Dore Granite pluton. Evaporitic horizons are not known from the Maronan Supergroup, but thrusting of Soldiers Cap Group over the Staveley and Doherty Formations, known to have contained such rocks, is likely (Chapter 3). An evaporite-derived, metamorphic component is therefore possible. Retrograde reactions are also possible, since hydrothermal fluid movement was occurring along major fault zones during the waning stages of the regional thermal event.

Classification of the hydrothermal fluid as magmatic or metamorphic may be an artificial distinction. In regionally metamorphosed terranes, there is commonly a close genetic link betwen prograde metamorphism, with attendant dehydration, and the generation of anatectic granitoids (*e.g.* Whitney, 1988; Clemens, 1992). The "metamorphic" fluid in these instances is initially dissolved in the magma, to be released at higher crustal levels as "magmatic" fluid when the magma reaches vapour saturation.

As the hydrothermal fluid evolved, it became cooler and more dilute. Boiling cannot explain the distinct salt-undersaturation, and dilution of the primary fluid by mixing with a second, low salinity fluid is necessary. Meteoric water is an obvious candidate, but the expected trend towards lower $\delta^{18}O$ values is not observed. The oxygen isotopic signature retains a deep-crustal (positive $\delta^{18}O$) character, and carbon and deuterium data are consistent with this source. Meteoric fluid could perhaps have acquired a deep-crustal isotopic character through extensive interaction at high temperature with volumetrically dominant metamorphic or igneous rocks before mixing with the primary fluid. This is possible if the Mount Dore and related faults extended to the surface, but seems improbable, leaving only the option of introduction of at least one other deep crustal fluid into the Mount Dore Fault Zone. If biotite δD data reflect those of the evolved fluid, this second fluid was probably metamorphic.

As faulting and uplift progressed, downward percolating meteoric waters clearly affected the mineralization, producing a supergene oxide zone and underlying chalcocite blanket. Hydrothermal alteration does not record this event, however.

6.6 CONCLUSIONS

Fluid inclusion and alteration geochemical data record the existence of an early, hot ($\geq 500^{o}C$), highly saline (up to 70 wt% dissolved NaCl, KCl, $CaCl_2$, $FeCl_2$, $MgCl_2$) hydrothermal fluid, probably with a considerable CO_2 content, which evolved towards a cooler, less saline, CO_2-poorer composition. Phase immiscibility occurred early in the history, producing a more saline, H_2O-rich phase which remained in the system, and a CO_2-rich phase which apparently escaped. Boiling may have been occurring sporadically later in the history.

The trend in fluid composition can only be explained by mixing of the primary fluid with at least one other low-salinity fluid. Oxygen, deuterium and carbon isotopic signatures indicate that both fluids were of deep-crustal origin, and at least one was metamorphogenic. Cooling probably occurred by adiabatic expansion into dilatant regions of the Mount Dore Fault Zone, and conduction of heat into the surrounding wall-rocks.

Meteoric waters interacted with the Mount Dore deposit at a very late stage, producing the oxide zone and chalcocite blanket presently capping the primary sulphide zone.